Synthetic Materials: Processing and Surface Modifications for Vascular Tissue Engineering

William E. King III, Benjamin A. Minden-Birkenmaier, and Gary L. Bowlin

Contents

1 Introduction 138
1.1 Ideal Mechanical Properties 140
2 Synthetic Polymers 140
2.1 Non-resorbable Polymers 142
2.2 Bioresorbable Polymers 146
3 Methods of Fabrication 156
3.1 Knitting and Weaving 156
3.2 Electrospinning 158
3.3 Sponges 160
4 Surface Modification 161
4.1 Methods of Surface Modification 161
4.2 Materials of Surface Modification 169
5 Conclusions 177
References 177

Abstract

Cardiovascular disease is a prominent issue in developed countries, notably the United States, and is expected to further escalate. As a result, the demand for "off the shelf" vascular grafts will concurrently increase. These readily available grafts for large vessels (>6 mm) are already on the market in the United States and Europe, but reliable products for small diameters vessels have eluded researchers and industry alike. In this chapter, the ideal attributes of a small diameter vascular graft are considered. Prominent synthetic polymers, subdivided into non-resorbable and resorbable, used in vascular grafts are covered. Each polymer's history, bulk mechanical properties, degradation mechanisms, and notable

W. E. King III · B. A. Minden-Birkenmaier · G. L. Bowlin (✉)
Department of Biomedical Engineering, University of Memphis, Memphis, TN, USA
e-mail: wkingiii@memphis.edu; bmndnbrk@memphis.edu; glbowlin@memphis.edu

B. H. Walpoth et al. (eds.), *Tissue-Engineered Vascular Grafts*, Reference Series in Biomedical Engineering, https://doi.org/10.1007/978-3-030-05336-9_2

implementation by researchers are discussed, followed by significant methods of fabrication to construct vascular grafts out of these materials. Subsequently, methods to modify graft surfaces and the materials that can be used to modify these surfaces are covered.

1 Introduction

Each year, more than 17 million people worldwide die from cardiovascular disease, accounting for nearly 20% of all deaths in 2015, and is projected to rise to nearly 24% of all deaths in 2030 (World Health Organization 2013). Many of these cases involve atherosclerotic narrowing of arteries which interferes with the perfusion of vital organs, causing ischemic events that damage or destroy precious tissues. Arteries blocked in this way are often replaced surgically, with approximately 400,000 coronary artery bypass surgeries performed within the United States in 2016 (Alexander and Smith 2016). Autologous sources of vascular replacements are often limited because of disease or the necessity for multiple replacements per patient; therefore, there is a need for vascular substitute materials that can serve as long-term vascular grafts. Early attempts at developing these materials involved tubes constructed from silk, metal, nylon, glass, and ivory, which were quickly occluded by thrombosis (Greenwald and Berry 2000; Xue and Greisler 2003). The discovery of the polymeric materials polyethylene terephthalate (PET, commonly referred to as Dacron) and expanded polytetrafluoroethylene (ePTFE, commonly referred to as Gore-Tex) became commercial successes as the Food and Drug Administration (FDA) approved vascular grafts. These materials work adequately for grafts with inner diameters larger than 6 mm, but smaller diameters experience high failure rates. Acutely these grafts fail via thrombosis while chronically they fail through hyperplasia and infection (Abbott et al. 1987; Greenwald and Berry 2000; Salacinski et al. 2001). Hyperplastic failure can be further divided into intimal hyperplasia occurring at the midgraft and anastomotic hyperplasia occurring around the suture site. Hyperplasia is a reactive cellular change due to insult or injury. Thus, there is a further need to develop biomaterials with optimal tissue-material interactions that can succeed in these small diameter graft applications.

Physiology determines the design criteria. The ideal vascular graft, especially for small diameter applications, must embody numerous design criteria in order to be successful (Table 1).

The ideal vascular graft must have mechanical properties close to that of the native vessel, namely circumferential and longitudinal compliance, while having equal to or

Table 1 Ideal attributes of a synthetic vascular graft

Ease of surgical handling	Infection resistant	Flexible
Durable during tissue ingrowth	Biocompatible	Non-thrombogenic
Suture retention	Kink resistant	Porous while leak resistant
Matched compliance of native artery	Resistant to aneurysm formation	Off the shelf/readily available

superior burst strength. Failure to match the compliance of small diameter grafts with the perianastomotic vasculature will result in thrombosis, aneurysm dilatation, and hyperplasia (Brossollet 1992; Greenwald and Berry 2000; Klinkert et al. 2004; Wise et al. 2011). Furthermore, it must resist collapsing or forming kinks while maintaining flexibility. The material should also be biocompatible, which encompasses both the bulk material and any leachables. The ideal vascular graft should be porous enough to allow for cell and capillary ingrowth to facilitate tissue regeneration (Walpoth and Bowlin 2005). In order to best achieve tissue regeneration, vascular grafts need to be replaced by native tissue over time to facilitate new, functional tissue formation. The process of dissolution of a biomaterial in vivo is termed biodegradation. If the degradation products are among those naturally processed in the body, the dissolution of these materials is termed bioresorption.

The ideal bioresorbable vascular graft should create a favorable environment for cellular ingrowth and remodeling. Immediately after a biomaterial is implanted, blood proteins such as albumin, fibrinogen, and IgG begin to adsorb onto the surface of the material in a phenomenon known as the Vroman effect. In this process, high mobility proteins adsorb first and are gradually replaced by low mobility proteins with higher surface affinity (Vroman and Adams 1969). The initial surface chemistry will determine the composition of the new protein surface and consequently set the stage for cellular interactions. Subsequently, platelets begin to adhere to the material followed by nucleated cells. The first nucleated cell to respond to the foreign material is the neutrophil, followed then by macrophages and other immune cells. Next, endothelial cells, smooth muscle cells, and their progenitors migrate into the graft. In many animal models, the endothelial cells and smooth muscle cells migrate inwards from the anastomosis of the native vessels into ends of the graft in a process known as trans-anastomotic ingrowth. Trans-anastomotic ingrowth is sufficient in many animal models, but reliance on this type of migration in humans limits the practical length of a graft that can be used. After months of implantation, ingrowth is limited to millimeters (Davids et al. 1999; Zilla et al. 2007). As an alternative mode, cell ingrowth can occur through transmural migration, and in this process, capillaries grow into the exterior walls of the vessel or graft to source progenitor cells. It is hypothesized that this mode of regeneration will be required as the primary mechanism in humans (Row et al. 2015). Through these mechanisms, the ideal vascular graft would allow for the growth of endothelial cells to develop a layer that contacts the blood and communicates with the surrounding cells via signaling mechanisms. The formation of this cellular neointima would be non-thrombogenic, infection resistant, and curtail intimal hyperplasia. It has been reported that pores between 18 and 50 μm in diameter promote endothelial cell attachment and neointima formation (Mathews et al. 2012; Matsuda and Nakayama 1996; Narayan and Venkatraman 2008). Evidence suggests that the disruption of this endothelial cell layer signaling is a major factor in intimal hyperplasia and graft failure, thus its development and maintenance are paramount (Jeschke et al. 1999; Melchiorri et al. 2013). For a bioresorbable vascular graft approach, the material should be biodegraded at a specific rate, so that as

cells infiltrate and make their own extracellular matrix, the construct will be replaced without loss of mechanical performance. This would result in no extraneous material left in the body and a reconstructed native vessel that would maintain itself.

1.1 Ideal Mechanical Properties

The primary mode of chronic vascular graft failure is thought to be compliance mismatch (Abbott et al. 1987; Salacinski et al. 2001). The sites of anastomosis in a vascular graft always experience a decrease in diameter and a decrease in compliance due to the nature of the graft material and suturing technique. Inexplicably, the region of a few millimeters on either side of the suture experiences a significant increase in compliance. This region is referred to as the para-anastomotic hyper-compliance zone (PHZ). In detail, the region proximal to the anastomotic suture has a high mean shear stress and relatively low oscillation compared to the mean, while the distal region has a low mean shear stress with a high degree of oscillation. This circumstance gives rise to anastomotic hyperplasia through three proposed mechanisms: (1) excess mechanical stress leads to wall injury, (2) excessive cyclic stressing activates smooth muscle cells to proliferate and produce ECM, and (3) the increased compliance regions result in increased stasis of blood solutes (Bassiouny et al. 1992; Salacinski et al. 2001; Sottiurai et al. 1988; Stewart and Lyman 1992). It is therefore paramount to design novel vascular grafts that closely match native arterial compliance in order to prevent the formation of a PHZ zone, resulting in anastomotic hyperplasia and failure. In the literature, numerous studies have measured the mechanical properties of human vessels to serve as a reference for the creation of man-made grafts. Due to the inhomogeneity of human physiology and variations in testing protocols, no single value exists for vessel compliance or any other mechanical properties. Furthermore, the primary recipient population for vascular grafts are those with poorly functioning vessels. As a result, those vessels will have distinctly different trends in mechanical properties than their healthy counterparts, posing a further challenge to researchers. Currently, the only option researchers have is to use the reported properties of native vessels (Table 2) as a guideline and observe the results of future human clinical trials.

2 Synthetic Polymers

From the criteria of an ideal vascular graft, there are currently a limited number of materials that can be implemented in vivo. This book chapter covers the foremost synthetic materials that have been used as the primary mechanical structure in vascular grafts. Afterwards, prominent surface modification techniques to improve performance are covered.

Table 2 Reported mechanical properties of notable human blood vessels. (*C* circumferential, *L* longitudinal)

Type of blood vessel	Elastic modulus (MPa)	Ultimate tensile stress (MPa)	Strain at failure (%)	Burst pressure (mmHg)	Compliance	Suture retention strength (gf)	References
Saphenous vein	C: 2.3–42.6 L: 23.7–130.2	C: 4–10.5 L: 27.4	C: 2–242 L: 17–83	1,300–3,900	0.7–1.5%/ 80–120 mmHg	196–255	Donovan et al. 1990; Konig et al. 2009; L'Heureux et al. 2006; Seifu et al. 2013; Soletti et al. 2010; Stekelenburg et al. 2009
Internal mammary artery	C: 8.0 L: 16.8	C: 4.1 L: 4.3	C: 134 L: 59	1,599–4,225	4.5–6.2%/ 80–120 mmHg 11.5%/ 100 mmHg	138–200	Konig et al. 2009; L'Heureux et al. 2006; Stekelenburg et al. 2009
Femoral artery	C: 9–12	C: 1–2	C: 63–76	N/a	N/a	N/a	Fung 1984; Yamada 1970
Carotid artery	C: 5.7 L: 2.4	C: 2.6 L:0.95	C: 125 L: 105	N/a	N/a	N/a	McKenna et al. 2012

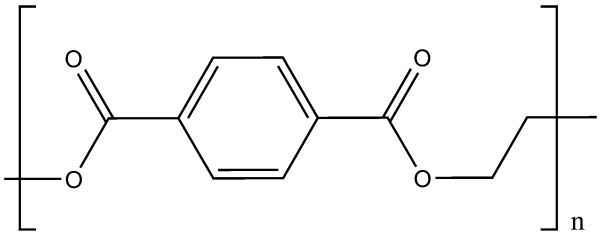

Fig. 1 Monomer structure of poly(ethylene terephthalate)

2.1 Non-resorbable Polymers

2.1.1 PET [Poly(Ethylene Terephthalate)]

A number of non-resorbable polymers have been used to construct vascular grafts, with varying success. Poly(ethylene terephthalate) (PET, Fig. 1), commercially best known as Dacron, was first used in 1957 as a successful nonbiological vascular graft material (Hess 1985). The bulk properties of PET include a fiber-oriented tensile strength of 170–180 MPa and a tensile modulus of 14 GPa (Lawton and Ringwald 1989). Dacron is hydrophobic, reducing the ability of endothelial cells to adhere to the surface (Dekker et al. 1991). PET threads are either knitted or woven; woven grafts have minimal porosity and creep, while knitted grafts are more porous and distend further in the radial direction. The knitted grafts are often pre-clotted with gelatin, collagen, or albumin before implantation to reduce leakage of blood through the graft (Cziperle et al. 1991; Jonas et al. 1988; Scott et al. 1987). Both the knitted and woven grafts are reinforced with flexible rings to improve the resistance of the graft to the compressive forces created by the surrounding tissue (Xue and Greisler 2003). As a biostable polymer, Dacron grafts can last over 10 years in the body without deteriorating, with no significant differences in graft patency between the knitted and woven grafts (Quarmby et al. 1998). Unlike the ideal vascular graft, Dacron grafts do not facilitate significant cellular infiltration but alternatively use adherent proteins to form the blood-contacting layer. In the first several hours after implantation, a layer of platelets, fibrin, lipoprotein, IgG, albumin, and cells from circulating blood builds up on the luminal side of the graft, compacting into a permanent coagulum over a period of months (Davids et al. 1999; Dekker et al. 1991). On the extramural side of the graft, a layer of foreign body giant cells forms outside the graft wall, which is then surrounded by a fibrous tissue capsule that walls off the graft from the rest of the body. Due to the reliance on cellular migration from the ends of the graft, Dacron grafts typically have an acellular midgraft fibrin layer (Xue and Greisler 2003).

2.1.2 ePTFE [Expanded Polytetrafluoroethylene]

Expanded polytetrafluoroethylene (ePTFE), commercially best known as Gore-Tex, is a material derived through a post-processing modification of polytetrafluoroethylene (PTFE, Fig. 2) (Shalaby 1996). ePTFE is the only current synthetic clinical alternative to Dacron vascular grafts and has been used in vascular grafts since the 1970s (Gandhi et al. 1993; Ravari et al. 2010). Specifically, ePTFE

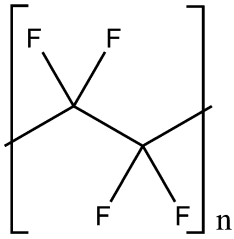

Fig. 2 Monomer structure of polytetrafluoroethylene

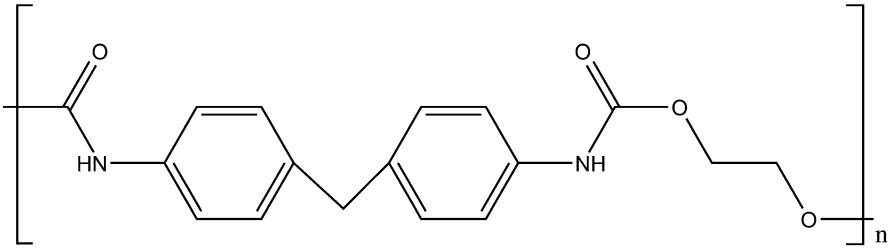

Fig. 3 Representative structure of a polyurethane monomer

grafts are created by stretching and expanding tubes of polytetrafluoroethylene to create small pores defined by nodes and fibrils. The expanding process can be highly tailored to give consistent, controllable pore sizes. Thus, mechanical properties and porosity are highly variable for the given application. The preprocessed material, PTFE, has a tensile modulus of elasticity of 0.5 GPa and a tensile strength of 14 MPa (Lee et al. 1995). Polytetrafluoroethylene does not biodegrade within the body, meaning that these grafts are non-resorbable, and its electronegativity minimizes the adherence of blood proteins to the luminal surface (Xue and Greisler 2003). Nevertheless, upon implantation, a fibrin/platelet layer develops on the luminal surface of the graft which, like the Dacron graft, is acellular in the midgraft region (Bellon et al. 1996; Sottiurai et al. 1983). Failure rates of both the Dacron and ePTFE grafts are similar regardless of implantation site, but the success of these grafts is higher in areas of high-velocity blood flow such as the aorta (Friedman et al. 1995; Polterauer et al. 1992; Prager et al. 2001). In general, these synthetic grafts have lower patency rates than grafts fashioned of autologous venous tissue (Friedman et al. 1995; Green et al. 2000; Post et al. 2001). It is thought that the noncompliant nature of both ePTFE and Dacron is an underlying cause of graft failure, because it creates unusually high stresses at the juncture of the graft and the more compliant native tissue (Salacinski et al. 2001).

2.1.3 PU [Polyurethane]

The use of polyurethane (PU, Fig. 3) as a blood-compatible biomaterial was first notably explored by Boretos et al. in the late 1960s (Boretos and Pierce 1968). In order to address concerns about compliance mismatch between graft and native vessel, a significant amount of research has been invested in PUs as vascular grafts.

PU's low elastic modulus, increased compliance, and closer match in mechanical properties to the properties of native vessels mark it as a potential improvement over Dacron and ePTFE (Bos et al. 1998; Wang et al. 2007). On the molecular level, three domains comprise PUs: a "soft" domain (usually polyol), an "extending" domain, and a diisocyanate "hard" domain. The sizes of these domains can be controlled during the formation process to modify the properties of the final product. For instance, using longer polyol "soft" chains makes the final product more elastic, while increased crosslinking via increasing the ratio of "hard" to "soft" domains creates a more rigid product (Guo et al. 2007; Sarkar et al. 2007; Soto et al. 2014). Thus, the radial compliance of a PU graft can be controlled to more closely match the compliance of the native vessel to which the conduit will be sutured, minimizing the potential for intimal hyperplasia. The material tailorability results in a wide range of material properties with a tensile strength of 20–50 MPa and a tensile modulus of 5–1150 MPa (Coury et al. 1988). Additionally, PUs have been shown to seal themselves around punctures, such as those created when a vascular graft is stitched to the end of a native artery, and have low thrombogenicity (Edwards et al. 1995; Seifu et al. 2013).

Despite the promising in vivo results of PUs as vascular grafts in animals, their first clinical trial in the 1990s was aborted due to 8 of 15 grafts becoming completely occluded due to kinking, deterioration, and anastomotic mismatch (Zhang et al. 1997). Subsequent examinations concluded that the polyester polyols used to create the PUs degraded hydrolytically, contributing to unexpected degradation of the grafts (Santerre et al. 1994). Polyether groups were then substituted for the polyester groups to create new trial PUs, but while these materials avoided hydrolysis, they were more vulnerable to oxidative degradation, rendering them equally ineffective. A PU made from polyetherurethaneurea had some success when used as a vascular access graft, although these grafts required more frequent endovascular intervention relative to the transposed brachial-basilic fistula controls (Kakkos et al. 2008).

More recently, PUs made from polycarbonate have been investigated. These PUs are not susceptible to hydrolytic or oxidative degradation and have improved rates of endothelialization relative to ePTFE grafts in a rat aorta model (Jeschke et al. 1999). However, canine model trials of polycarbonate-based PU grafts have shown varying results. One study of a Dacron-reinforced polycarbonate-based PU tube demonstrated a high degree of thrombus formation when used as an abdominal aorta replacement, while another study using poly(carbonate-urea)urethane tubes as canine aorta-iliac replacements reported little-to-no thrombogenicity (Seifalian et al. 2003; Xie et al. 2010). The second graft had the advantage of a microporous honeycomb structure lining the luminal surface which allowed for endothelial cell attachment; after 18 months in vivo, the explanted grafts had extensive collagen deposition and endothelialization covering the luminal surface (Seifalian et al. 2003). This tissue ingrowth prevented both intimal hyperplasia at the anastomoses and delamination of tissue from the luminal surface, which have been demonstrated as frequent causes of graft thrombosis in PU grafts without a porous luminal structure (Marois et al. 1993; Martz et al. 1988). As such, poly(carbonate-urea)

urethane tubes incorporating this microporous honeycomb structure represent a significant improvement over previous attempts.

Further exploration of PUs involved using siloxanes such as poly-(dimethylsiloxane) as the soft segment, as these formulations are also resistant to degradation through hydrolytic or oxidative mechanisms (Gunatillake et al. 2003). In a 2010 study, Soldani et al. constructed 5 mm inner-diameter grafts using a siloxane-based PU blend (Fig. 4) which were then used to replace sections of the sheep's common carotid arteries over a period of 24 months. All of these grafts remained patent and free of occlusion for the entire 24-month period. These findings represented a significant improvement over the ePTFE controls (Fig. 5), half of which became completely occluded in as little as 6 months. After 6 months, a homogeneous neointima was observed in the siloxane-PU grafts, while the neointima of the ePTFE grafts was described as "patchy," and unlike the ePTFE grafts, the siloxane-PU grafts showed no signs of calcification. Calcification is a pathologic process which results in stiffening and ultimately contributes to the failure of a graft.

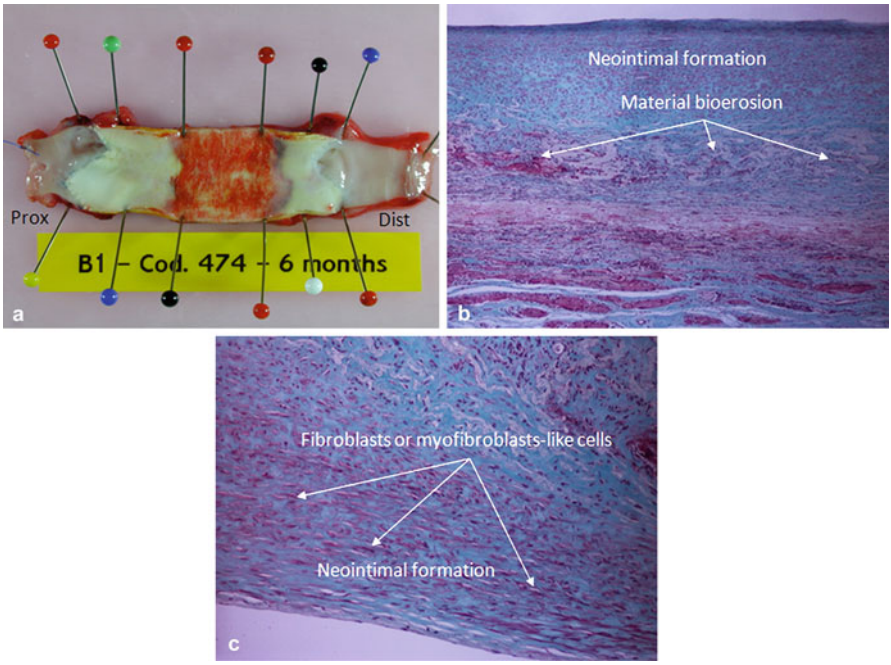

Fig. 4 (**a**) Siloxane-PU graft 6 months after implantation. Note neointima partially covering luminal surface extending inward from the anastomoses. (**b**) Histological section near proximal anastomosis showing thick neointimal formation, with arrows pointing to the front of the resorption. Lumen is at the top. (**c**) Close-up of neointimal formation near distal anastomosis, showing fibroblast or myofibroblast-like cells. Lumen is at bottom left. (Reprinted from Biomaterials 31:2592-2605, Soldani et al., Long term performance of small-diameter vascular grafts made of a poly (ether) urethane–polydimethylsiloxane semi-interpenetrating polymeric network, Copyright (2010), with permission from Elsevier)

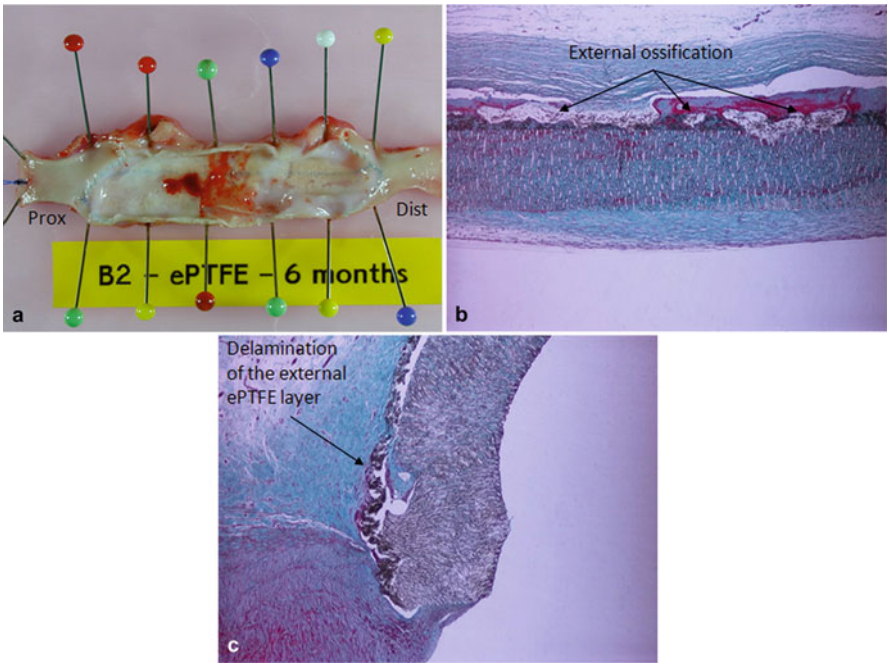

Fig. 5 (**a**) ePTFE graft 6 months postimplantation. Note the thin, patchy neointima and the thrombus formation midgraft. (**b**) Histological section of ePTFE graft near proximal anastomosis showing ossification and thin neointimal capsule on graft lumen. (**c**) Histological section of ePTFE graft near distal anastomosis, showing delamination of ePTFE and limited perigraft tissue infiltration, with no neointima visible on lumen. All sections stained with Masson's trichrome staining. (Reprinted from Biomaterials 31:2592-2605, Soldani et al., Long term performance of small-diameter vascular grafts made of a poly (ether) urethane–polydimethylsiloxane semi-interpenetrating polymeric network, Copyright (2010) with permission from Elsevier)

However, the siloxane-PU grafts had a higher level of surrounding fibrovascular tissue which could potentially limit their long-term distensibility and compliance. It is important to note though that post-explantation mechanical properties were not tested. Moreover, the siloxane-PU grafts had slower rate of endothelialization than the ePTFE grafts, with endothelial cells migrating from the proximal and distal segments. This reduced rate was theorized to be a result of a dense fibro-lamellar layer formed on the outside of the graft, which blocked capillary infiltration from the perigraft tissue (Soldani et al. 2010). Future iterations of this graft with a more porous outer layer may be more successful with endothelialization.

2.2 Bioresorbable Polymers

A prevailing bioresorbable graft strategy is to use a slowly degrading polymer so that as cells infiltrate the graft and produce their own extracellular matrix, the

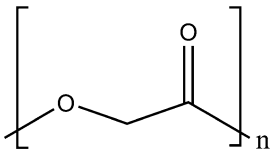

Fig. 6 Monomer structure of polyglycolic acid

polymer can slowly be removed, i.e., hydrolysis and replaced with natural tissue. Such biodegradation must be carefully tuned so as not to weaken the graft before enough load-bearing natural tissue is present. Thus, research has focused on developing grafts out of polymers and polymer blends whose degradation can be finely controlled.

2.2.1 PGA [Polyglycolic Acid]

Polyglycolic acid (PGA, Fig. 6) is a rigid thermoplastic first employed in the medical field as suture material in 1962 under the trade name Dexon (Gilding and Reed 1979). The polymer has a high degree of crystallinity at 46–50%, is hydrophilic, and has a tensile strength of 12.5 GPa (Pathiraja and Adhikari 2003; Ulery et al. 2011). PGA is not soluble in most organic solvents and is rapidly degraded hydrolytically. Specifically, the degradation mechanism occurs in two steps. First, water diffuses in into the amorphous regions of the polymer and results in hydrolytic chain scission of the ester groups. Second, the degradation of the crystalline regions of the polymer occurs (Pathiraja and Adhikari 2003). The degradation product glycolic acid is a component of the citric acid cycle and is readily processed in vivo. This process occurs rapidly and results in a loss of mechanical strength over 2–4 weeks (Pachence and Kohn 1997).

In 1982, Greisler et al. studied how PGA grafts behaved in a rabbit animal model. The grafts consisted of woven PGA with a fiber diameter of 3.5 mm and a longitudinal suture made of 6-0 polypropylene to form a cylinder. The weave of the graft had a pore size of 400 μm and a filament diameter of 250 μm. Under anesthesia, rabbits had 24 mm of infrarenal aorta resected and replaced with a graft. Forty-five rabbits were sacrificed and evaluated between 2 days and 7.5 months. The study showed the degradation of the grafts between 3 weeks and 2 months. Seventy-six percent of the graft specimens show parallel walls with the original 3–4 mm internal diameter. Eleven percent of the grafts showed moderate true aneurysmal dilatation (5–10 mm). Thirteen of the grafts showed severe intimal hyperplasia. One-month postimplantation revealed that the luminal surface was lined with a confluent layer of cells that had the morphology and functionality of endothelium (Greisler 1982). The authors note that the rabbit model is limited in external validity in that human pannus ingrowth is limited to approximately 1 cm at each anastomotic site. Due to PGAs rapid degradation timescale, PGA is frequently used as a copolymer to alter its properties.

2.2.2 PLA [Polylactic Acid]

Polylactic acid (PLA, Fig. 7) was discovered in 1932 by Wallace Carothers at DuPont. It was not until 1971 that Kulkarni et al. published about using PLA

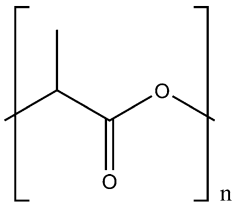

Fig. 7 Representative structure of a polylactic acid monomer

polymers for biomedical applications (Kulkarni et al. 1971). PLA is composed of lactic acid which is a chiral molecule with two enantiomers: L- and D-lactic acid (Lopes et al. 2012). As a polymer, PLA is a linear aliphatic polyester widely used in the medical field. The mechanical properties of PLA can widely vary based off of average molecular weight and degree of crystallinity. The tensile strength of poly-L-lactide (PLLA) can range from 55 to 59 MPa, while annealed PLLA tensile strength can vary between 47 and 66 MPa (Perego et al. 1996). Similarly, poly-DL-lactide (PDLLA) tensile strength can range from 40 to 44 MPa. The trend follows that a higher molecular weight results in a greater tensile strength (Perego et al. 1996). PLA degrades via simple hydrolysis of the ester backbone in vivo to yield lactic acid, a biological metabolite (Jamshidian et al. 2010). As a result, PLA is cleared from the body leaving no foreign material left behind.

In order to solve the compliance mismatch issue seen with PLA vascular grafts, Bagnasco et al. electrospun 5 mm diameter PLLA vascular grafts. In addition, ovine femoral arteries were harvested to serve as an experimental comparison. Both grafts and ovine arteries were subjected to physiologic pulsatile pressures of 50–90, 80–120, and 100–150 mmHg at 60–80 beats per minute. Pressure and diameter were measured to obtain compliance and elastic modulus. At 80–120 mmHg, the average compliance of the PLLA grafts was $0.93 \times 10^{-2} \pm 0.13 \times 10^{-2}$ mmHg while the ovine artery was $0.79 \times 10^{-2} \pm 0.20 \times 10^{-2}$ mmHg in a pressure range of 100–130 mmHg (Bagnasco et al. 2014). The authors showed that a bioresorbable vascular graft could be constructed with a compliance closely approximating that of native artery. In practice, due to its mechanical properties as a brittle polymer and its degradation rate, PLA is almost exclusively incorporated as a copolymer.

2.2.3 PCL [Poly(ϵ-capralactone)]

Poly(ε-caprolactone) (PCL, Fig. 8) was first synthesized by the Carothers group in the 1930s and has since been extensively studied as a bioresorbable polymer. PCL is often used as a suture material, drug delivery device, and root canal filling, among other applications (Woodruff and Hutmacher 2010). PCL is a hydrophobic, semicrystalline polymer that is soluble in many organic solvents and insoluble in alcohols and water (Ulery et al. 2011). Due to its low melting point, around 60 °C, PCL is easily manipulated into a variety of forms. PCL has a bulk tensile strength of 23 MPa and an elongation at failure of >700% (Gunatillake et al. 2006).

In vivo, its degradation first occurs through a hydrolytic cleavage of its poly(α-hydroxy) ester bond. This cleavage releases nontoxic segments with molecular weights under 30,000 Daltons that are then phagocytosed by macrophages and

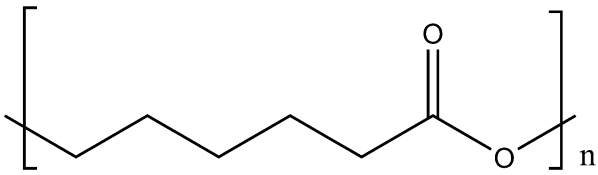

Fig. 8 Representative structure of a poly(ε-caprolactone) monomer

enzymatically degraded in phagosomes (Chen et al. 2000; Sivalingam et al. 2003; Sivalingam et al. 2004). This degradation process is generally slower than the degradation of PGA, PLA, or poly(lactic-co-glycolic acid) (PLGA) with a degradation timescale of 1–3 years (Ulery et al. 2011). PCL degradation is dependent on the molecular weight (MW) of the polymer, with a higher MW degrading more slowly, thus affording some control over degradation rates (de Valence et al. 2012). PCL is often combined with other polymers to create composite graft materials with a shorter presence in vivo.

Zhu et al., in a 2015 study, created a bilayer vascular graft with an inner layer of wet-spun, circumferentially aligned PCL microfibers surrounded by an outer layer of electrospun PCL nanofibers. The inner microfiber layer promoted circumferential alignment in seeded vascular smooth muscle cells, while the large diameter of these fibers, 18.26 ± 6.13 μm, created interconnected macropores with a diameter of 27.04 ± 9.05 μm, which allowed for cellular infiltration. The outer layer of randomly aligned electrospun nanofibers, fiber diameter of 0.65 ± 0.46 μm, provided strength and elasticity by doubling the burst pressure of the graft to approximately 1200 mm Hg and tripling the elastic modulus to approximately 1.6 MPa. The grafts were implanted into an abdominal aorta rat model and had extensive endothelial cell and smooth muscle cell penetration with circumferential alignment after 2 weeks. This effect became more pronounced over the 12-week terminal time point (Zhu et al. 2015).

In order to study how small diameter PCL vascular grafts performed against ePTFE in a rat model, Pektok et al. electrospun fifteen 2 mm diameter grafts out of $M_n = 80{,}000$ g/mol PCL. Thirty rats had 1 cm of abdominal aorta resected. Fifteen rats received the PCL grafts and 15 received the ePTFE graft. Rats were sacrificed at 3, 6, 12, 18, and 24 weeks for graft evaluation. At 12 weeks, the PCL grafts showed confluent endothelial coverage, while at 24 weeks, the ePTFE were incompletely covered (Pektok et al. 2008). Starting at 3 weeks, the PCL grafts saw neoangiogenesis with cellular infiltration, while the ePTFE grafts did not have angiogenesis. During the entire study, the PCL grafts had a 100% patency rate with no aneurysmal dilatation. While these results are promising, there is a significant issue with external validity with vascular models to human. Nevertheless, PCL does show a significant improvement compared to the ePTFE control.

2.2.4 PDO [Polydioxanone]

Polydioxanone (PDO, Fig. 9) polymer was first synthesized in 1977 from p-dioxanone monomer by Doddi et al. Since then, PDO has seen commercial success as the suture material "PDS II," and due to its mechanical properties

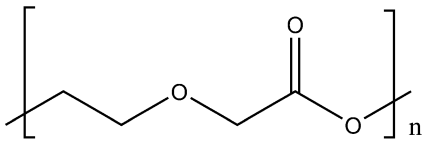

Fig. 9 Representative structure of a polydioxanone monomer

and degradation rates, researchers have begun investigating this polymer as a building material for tissue templates. PDO suture has a tensile strength of 552 MPa, Young's Modulus of 1.72 GPa, and an elongation to break of 30% (Bezwada et al. 1998). PDO degradation occurs through hydrolysis of its ester bonds with an average in vivo degradation rate of 6 months (Bezwada et al. 1998). The presence of an ether oxygen within its polymer chain backbone makes PDO more elastic than PLA or PGA (Boland et al. 2005).

In order to study PDOs use as a vascular graft, Greisler et al. in 1987 studied woven grafts of PDS suture in a rabbit model (Greisler et al. 1987). The distal infrarenal aorta was replaced with 24×4 mm inner diameter grafts and evaluated between 2 weeks and 1-year postimplantation for tissue thickness, prostaglandin content, compliance, and tensile strength. Over the course of 1 year, none of the grafts failed due to stenosis, although one developed true aneurysmal dilatation. After 3 months, the inner capsule thickness averaged approximately 420 μm, while data from previous studies with this group show PGA grafts had an average capsule thickness of 620 μm and Dacron grafts had 180 μm. Histologically, the grafts had a confluent layer of endothelial-like cells after 2 weeks, and after 1 month, the inner capsule consisted of circumferentially and longitudinally oriented smooth muscle cell-like myofibroblasts. The outer capsule showed vascularized connective tissue elements. By the 6- and 12-month time points, no PDS graft remained and all grafts still possessed endothelial-like confluent cells with a dense subendothelial matrix with minimal calcification. Prostaglandin data revealed that the endothelial-like layer on the PDS grafts produces 6-Keto-$PDF_{1\alpha}$, a metabolite of prostaglandin F normally produced by functional endothelial cells (Greisler et al. 1987). In addition, the authors looked at the ratio of 6-Keto-$PDF_{1\alpha}$ to thromboxane B_2 as a biomarker of relative thrombogenicity between PDS grafts, Dacron, and controls, indicating less thrombogenicity. The PDS group did not differ from the normal aorta control group, while the Dacron group showed a diminished ratio compared to control. These results suggest the nature of the material can affect the subsequent activity of cells. Lastly, the authors took the tissue/graft complexes of 2-month explanted grafts to evaluate mechanical properties. Grafts showed a 3.5 mm progressive increase in graft diameter after a systolic pressure range of 0–400 mmHg. Pressure changes beyond this point did not result in a measurable change in diameter. Grafts withstood 1250 mmHg of pressure without bursting and were not evaluated to failure. These results suggest that the graft/tissue complex behaves in a similar manner to native vasculature.

In another study in 2001, Teebken et al. compared woven grafts constructed from PDS suture, allogenic acellularized arteries seeded with autologous endothelial cells, and arterial autografts in German landrace pigs. Two centimeters of the common

carotid arteries were resected and replaced with one of the three grafts. Two groups (4 and 5 mm diameter) of PDS grafts were tested. Grafts were evaluated at 1 week or 4 months via ultrasound, angiography, and histology. At both 1 week and 4 months, all PDS groups had some stenosis or complete obstruction (Teebken et al. 2001). The grafts showed that the PDS fibers were surrounded by inflammatory cells (primarily macrophages), and the grafts had organized thrombi as well as intimal thickening. The decellularized graft group with a seeded endothelium had 11% of the grafts at 1 week completely patent and 43% completely patent at 4 months. The autograft group showed 100% patency at both time points. The authors conclude that PDS prostheses are unsuitable as small diameter grafts in at least the porcine model.

In a later study, Garg et al. studied human macrophage interactions on electrospun PDO vascular grafts. Cells were seeded on PDS, elastin, and PDO:elastin blends. Cells were seeded at 400,000 cells per well onto 10 mm discs of the vascular graft. Supernatants were collected at 7, 14, 21, and 28 days to be analyzed via ELISA. Results showed that growth factor secretion profiles for vascular endothelial growth factor (VEGF) and acidic fibroblast growth factor (aFGF) were similar across all samples by day 21 and 28 (Garg et al. 2009). Histological evaluation shows that scaffolds with high PDO:elastin ratios had cell infiltration. The authors concluded that high ratio PDO:elastin blends are conducive to tissue regeneration and angiogenesis. PDO's use as a biodegradable material for vascular grafts appears to be reliant on the material's preparation to guide the in vivo cellular response, but external validity in animal models versus humans obfuscates the exact nature of this response.

2.2.5 PGS [Poly(glycerol-sebacate)]

Poly(glycerol-sebacate) (PGS, Fig. 10) is a bioresorbable, thermoset elastomer that was first synthesized and used in biomedical applications in 2002 (Kemppainen and Hollister 2010; Wang et al. 2002). PGS has the bulk mechanical properties of a typical soft elastomer with a nonlinear stress-strain behavior. Due to this behavior, PGS can be thought of as a biorubber. Specifically, PGS has a tensile Young's modulus of 0.025–1.2 MPa, an ultimate tensile strength (UTS) of greater than 0.5 MPa and a strain to failure of at least 330% (Chen et al. 2008; Sundback et al. 2005; Wang et al. 2002). The biorubber is mildly hydrophilic with a water contact angle of 31.9°. The mechanical properties can be tailored based on the curing time

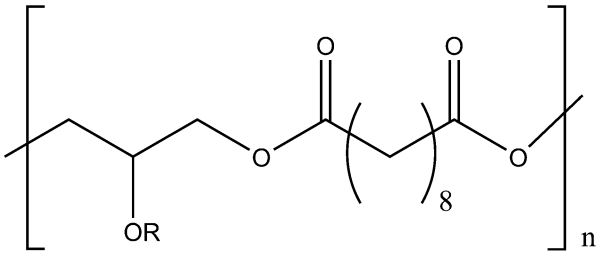

Fig. 10 Representative structure of a poly(glycerol-sebacate) monomer

and temperature as well as the ratio of glycerol to sebacate acid. It has been shown that PGS has shape memory behavior due to its fixed phase and amorphous phase regions (Cai and Liu 2008). PGS degrades via surface degradation where loss of mass and mechanical properties occurs simultaneously, as opposed to the usual, significant loss of mechanical properties before mass. Degradation specifically occurs through cleavage of the ester linkages. Studies in rat models show that PGS completely degrades within 60 days, but this can be modified based on degree of crosslinking.

Crapo et al. in 2009 studied the mechanical properties of PGS as a bioresorbable vascular graft (Crapo and Wang 2010). The group posited that PGS would be a material that solved the compliance mismatch issue seen with most current vascular grafts in the literature. Grafts were constructed by casting a PGS solution in a salt packed mold, where the salt functioned as a porogen. Three fabrication methods were used, varying the outer molds, all with an inner 5.28 mm heat-shrinkable mandrel. The mold was cured and immersed in multiple baths over 2 days to let the mold and salt dissolve. Grafts were then lyophilized and stored. The authors did not report final average graft diameter after processing. PGS grafts were compared to PLGA grafts constructed by the same method as well as segments of pig common carotid arteries. Porosity was evaluated via micro-computed tomography (CT) to be $84.6 \pm 0.6\%$. The vascular grafts were connected to a sterile flow through bioreactor, seeded with baboon arterial smooth muscle cells and evaluated for 10 days. Flow rate was started at 1.0 ml/min and increased to 10.0 ml/min on day 10. Graft samples were evaluated mechanically after manufacture as well as after 10 days of cell culture. PGS, PLGA, and porcine arteries were evaluated for five compression cycles to 50% strain. PGS and the artery segment showed elastic behavior, while PLGA experienced plastic deformation. The compressive elastic modulus was analyzed and PLGA grafts had a statistically greater modulus of 3–6 MPa than both PGS grafts and the porcine arteries. Porcine arteries had a statistically greater modulus than PGS grafts of approximately 220 MPa and 40–80 MPa, respectively. PGS and arterial compliance were found to be similar up to 50 mmHg. PGS grafts after 10 days of culture had a burst pressure of 27 ± 19 mmHg and uncultured grafts could not establish pressure due to their extensive porosity. After 10 days of culture, the smooth muscle cells found to be confluent on the luminal surface and the collagen and elastin content of the grafts were evaluated. PLGA had significantly more collagen than PGS constructs and similar amounts of soluble elastin. PGS grafts contained significant more insoluble elastin (approximately 35% of the porcine artery after 10 days of culture). Insoluble elastin in PLGA was not statistically different than the elastin from uncultured grafts. The results of this study using a new, seminal material were a promising start. The lack of sufficient burst pressure and difference in elastic modulus compared to native arteries are the primary challenges to be solved.

Two years later in 2011, Lee et al. from the same group further explored the use of PGS in small-diameter vascular grafts in vitro. Grafts were constructed in a similar manner as described above (Lee and Wang 2011). The vascular grafts were connected to a sterile pulsatile bioreactor, seeded with baboon arterial smooth

muscle cells and evaluated for 3 weeks. Flow pressure was pulsatile, gradually increase from 20 to 120 mmHg over the 2 weeks with a final pulsatile pressure range of 90–125 mmHg, and after 2 weeks the pressure was kept constant at 120 mmHg. Micro-CT results showed an average pore size of the grafts to be 23.3 ± 3.9 μm. Histology of the post-culture vascular grafts showed the smooth muscle cells had adopted a multilayered composition with circumferential orientation. Staining showed ECM proteins and circumferentially oriented elastin fibers. This study shows early promising results of PGS as a bioresorbable vascular graft. PGS demonstrates the ability to induced both collagen and insoluble elastin production by baboon smooth muscle cells compared to only collagen produced with other bioresorbable polymers. These results will need to be further evaluated for external validity in animal models and cultured human cells. Furthermore, mechanical properties, namely burst pressure, still present challenges to this material's use as a vascular graft. Copolymers incorporating PGS may prove to be a successful strategy.

2.2.6 Copolymers and Polymer Combinations

It is common practice for researchers to blend together polymers in order to combine the strengths of materials while simultaneously ameliorating their weaknesses. While there are infinitely many combinations of copolymers, this section will highlight a few representative examples.

Two of the most heavily investigated degradable polymers are PLA and PGA. Both polymers are saturated poly-α-hydroxy esters, but the extra methyl group of PLA makes it slower-degrading and slightly more hydrophobic than the hydrophilic PGA (You et al. 2005). PLA and PGA can be combined in copolymers of PLGA in various ratios, with the ratio determining the degradation speed (Pavot et al. 2014). A vascular graft constructed from an inner knitted PGA layer and an outer woven PLA layer showed success in a 2008 study by Torikai et al. when implanted into a porcine aorta model. No aneurysms or thrombi occurred over the 12-month period of the study, and histological examination showed an endothelialized layer as well as a neomedia with functional, vasoresponsive smooth muscle cells and vasa vasorum (Torikai et al. 2008). More recently, Sugiura et al. fabricated grafts with an inner layer of 50:50 poly(L-lactic-co-ε-caprolactone) and an outer layer of either PLA or a mixture of PLA and PGA fibers, and demonstrated that the faster degradation of the PLA/PGA mix helped prevent calcification of the graft. However, since these grafts were implanted as aortic conduits in mice, rather than larger animals, it remains to be seen whether these fast-degrading constructs can maintain their mechanical integrity in large animals with greater blood flows (Sugiura et al. 2017).

In a 2017 study by Li et al., a knitted PLA material was sprayed with a PCL solution to imbed the PCL matrix within the PLA material. Samples were created using meshes of high and low fabric density with PCL, as well as without PCL, and compared to ePTFE. The high fabric density composite graft had the highest elongation strength, suture retention strength, shear strength, and compression/recovery strength. Both composite grafts had higher burst pressure than human

saphenous vein and canine femoral artery, similar suture retention strength, and had a higher resistance to torsion than the ePTFE and non-composite PLA grafts, as well as a higher compliance. Other requirements, such as cellular infiltration, endothelialization rate, and biodegradation rate were not investigated, but the mechanical testing data indicated that the addition of the PCL matrix significantly improved the ability of the graft to withstand the mechanical forces necessary to act as a vascular graft (Li et al. 2017).

In a similar effort, Williamson et al. developed a composite vascular graft by wet-spinning PCL nanofibers to make an inner luminal surface, which was then surrounded by an electrospun PU layer. Unlike the study by Li et al., Williamson et al. focused on in vitro cell response rather than mechanical characterization. Endothelial cells showed good attachment to the luminal PCL surface, with the formation of a confluent cobblestone layer over a period of 7 days. PECAM-1, a characteristic endothelial cell membrane marker, was expressed once confluence was established, and von Willebrand factor (vWF), a coagulation protein specific to endothelial cells, was released in a controlled fashion following stimulation. These endothelial cells were also shown to respond to nitric oxide, an important vasodilator and inhibitor of platelet adhesion. Additionally, smooth muscle cells were able to attach and proliferate throughout the PU outer layer. The template was also examined as a drug-delivery device, using trypsin as a model. A large burst release was observed, followed by a lower sustained release continuing throughout the 48-h time period. The authors suggest that the fibers could be impregnated with TGF-β to stimulate wound repair and endothelialization of the graft after implantation (Williamson et al. 2006).

In a 1988 study, Greisler et al. constructed 4 mm inner-diameter woven vascular grafts from PDO and another, faster-resorbing polymer, polyglactin 910 (PG910). These grafts were then implanted into rabbit aortas for periods of 2 weeks up to 12 months. Histological examination showed the PG910 component was completely resorbed after 2 months, while the PDO component lasted longer but disappeared by 6 months. Only one graft suffered stenosis, with no grafts occluding or dilating into aneurysms. Within the first few weeks, a thin fibrin coagulum formed on the luminal surface of grafts with occasional areas of endothelialization. After 1 month, the luminal surfaces were almost entirely endothelialized, with myofibroblasts infiltrating into the middle of the graft, developing phenotypic characteristics of smooth muscle cells. Capillaries were also observed to infiltrate throughout the graft, with the rate of ingrowth happening inversely to the resorption of the polymer (Greisler et al. 1988). Although this early success was not replicated in large animal experiments, the study provides an early blueprint of the two-polymer strategy, in which multiple polymers with different resorption rates may support tissue ingrowth while maintaining longer-term mechanical stability.

More recently, Pan et al. created composite small-diameter grafts by co-electrospinning fibers of PCL and PDO onto a 2-mm diameter cylindrical mandrel (Fig. 11). These composite grafts had elastic moduli, maximum strain and tensile strength, and water contact angles in between the properties of PCL or PDO alone. Preimplantation degradation testing showed that the PDO fibers degraded between 2

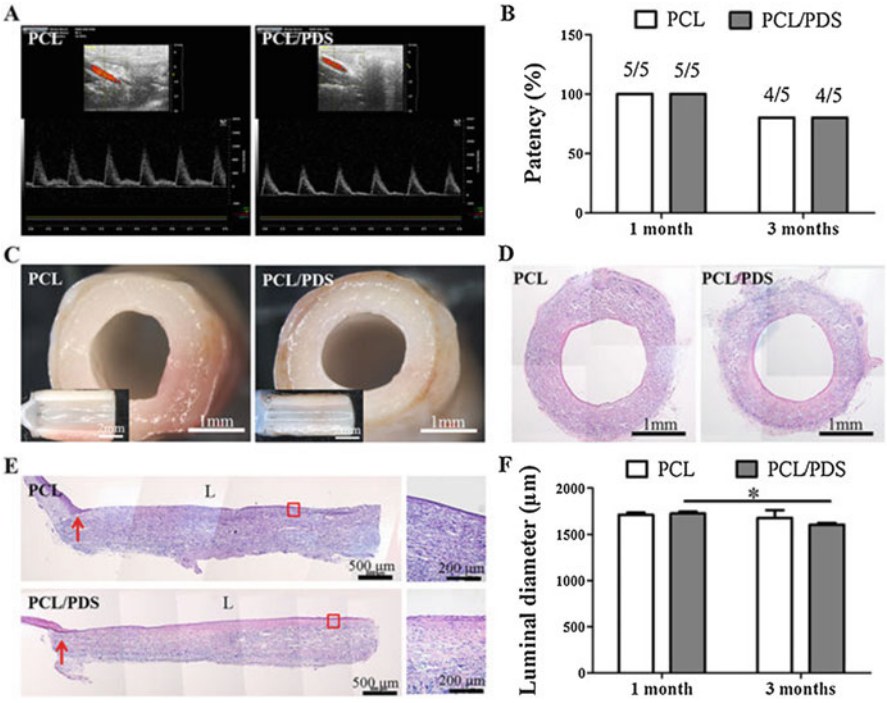

Fig. 11 Evaluation of the patency and luminal diameter of explanted grafts at 3 months after implantation. (**a**) The patency was measured by color Doppler ultrasound. (**b**) The patency rates of the PCL and PCL/PDS grafts at both time points. (**c**) The lumen of the explanted grafts was smooth and free of thrombus under stereomicroscope. (**d**) Cross sections were stained with H&E to identify the neointima formation. (**e**) Representative H&E staining of longitudinal sections of explanted grafts. (**f**) The luminal diameter of explanted grafts was calculated based on the cross sections with H&E staining. (**g**) Lumen; red arrows: suture site. $*p < 0.05$. (Reprinted from Scientific Reports, 7:3615, Pan et al., Small-diameter hybrid vascular grafts composed of polycaprolactone and polydioxanone fibers, 2017 with permission under Creative Commons CC BY license)

and 12 weeks, while the PCL fibers lasted throughout the entire 3-month study. As the PDO fibers degraded, they opened up larger pores within the structure that allowed for increased tissue ingrowth. Despite this degradation, no aneurysmal dilation was seen in these composite grafts when implanted into the abdominal aortas of rats. After 3 months, a complete neointima formed in both composite and PCL controls, but faster endothelialization and more collagen coverage was seen in the composite graft. While the PCL grafts had greater SMC infiltration at 1 month, at 3 months the composite graft had almost twice the amount of smooth muscle cells as the PCL control. Von Kossa staining showed no calcification of the graft walls. Anti-smooth muscle myosin heavy chain I showed that these smooth muscle cells contained the contractile elements necessary to functionally control vessel diameter. However, Masson, Safranin O, and Verhoeff-van Geison staining indicated that the pores formed by PDO degradation were not completely filled with new ECM after 3 months. Thus, future

iterations of this design should ideally use a sacrificial polymer with a slightly longer degradation period in order to better maintain the physical properties of the graft throughout the tissue infiltration process. It should be noted that physical properties of the grafts were not tested after explantation, so it is unknown whether they maintain the necessary strength and compliance to show success in a larger animal or human (Pan et al. 2017).

3 Methods of Fabrication

Many different fabrication methods have been mentioned in the examples covered earlier in this chapter. These fabrication methods have an extraordinary amount of impact on the overall mechanical properties and cell responses of the graft, and, as such, the choice of fabrication method is just as important as the choice of material when designing a vascular graft. This section serves to highlight the most common methods of fabrication for vascular grafts.

3.1 Knitting and Weaving

The techniques of knitting and weaving fibers have been around since early human existence and are reliable methods for creating 3D structures. As mentioned at the beginning of this chapter, the first vascular grafts were constructed out of woven or knitted materials (Linderman et al. 2014; Tomizawa 2014). Woven structures are created from two distinct sets of fibers that are then interlaced. Fibers positioned in the long axis are termed warps, while the lateral filling fibers are termed wefts (Akbari et al. 2016). The most common weaves are plain, satin, and twill. Different weaves can alter the mechanical properties of the structure, while the tightness of the weave will alter porosity. Woven grafts typically have great mechanical strength and minimal creep but are typically not very porous compared to knitted ones and can endure less in-plane force (Akbari et al. 2016). The greatest obstacle in these types of structures usually is inducing cellular adhesion and tissue ingrowth (Liao et al. 2013; Min et al. 2004). A typical strategy is to combine them with other nonwoven elements that can partially overcome this obstacle. A 2008 study by Torikai et al. investigated a vascular graft with an outer woven layer of PLA surrounding an inner PGA/collagen layer. After implantation into porcine aortas for 12 months, grafts showed no signs of thrombus or aneurysm, indicating good compatibility with blood as well as robust mechanical properties. Despite the typical issues woven grafts have with cellular infiltration, their grafts showed good SMC infiltration through the outer woven area, with corresponding collagen deposition (Torikai et al. 2008).

In contrast to woven grafts, knitted materials have greater porosity and distensibility, although their mechanical strength is still greater than that of most electrospun

materials. To form a knit, fibers are pulled through a previous loop to form a series of interconnected loops. The direction of the looping will determine if the knit is a weft or warp. A weft knit is defined as stitches of the same fiber arranged horizontally, while warp knits are arranged vertically. Different knits will give rise to differing mechanical properties. Weft knits have a greater degree of control over pore size, porosity, and overall fiber alignment, while warp knits have greater flexibility (Akbari et al. 2016). For these reasons, knits are often used to reinforce materials in vascular grafts. A 2015 study by Xie et al. examined composite grafts that combined several fabrication methods. First, a PLA yarn was weft-knitted into a tube, meaning that the entire piece of PLA fabric was knitted from just two long fibers. This knitted tube was then attached to a grounded mandrel, and a 50:50 copolymer of PCL and PLA (PLCL) was electrospun onto the knitted structure. The structure was then inverted so that the electrospun layer would be on the luminal side of the graft, and the graft was coated three times with a 1:1 solution of collagen and elastin. The collagen/elastin coating was then crosslinked with genipen to form a hydrogel. Additional grafts were created without the inversion, without the electrospinning, and without the collagen/elastin coating. Mechanical testing showed peak stresses of all constructs were between 11.0 and 13.0 MPa, with no significant differences between groups. All composite grafts showed greater burst pressure and suture retention strength than just knitted PLA. The grafts with the outer knitted PLA, inner electrospun layer, and collagen/elastin coating had the highest dynamic radial compliance, and this value was the closest to the compliance of native vasculature (Xie et al. 2016). To the authors' detriment, no cellular adhesion or infiltration studies were performed on these grafts, and it is unknown how the degradation of the respective polymer layers will affect graft performance.

In another study, Liu et al. created knitted templates of raw silk fibers, which were then treated with Na_2CO_3 to remove the immunogenic sericin from the core fibroin polymer. The templates were then submerged in a solution of sulfated, sericin-free silk fibroin and frozen for 12 h. Next, they were subjected to a freeze-drying process for 24 h to create a microporous sulfated silk sponge throughout the knitted vascular graft. Grafts were then treated with methanol to induce β-sheet formation in order to keep the silk in the sponges from dissolving out in aqueous environments. These grafts were shown to have significantly lower platelet and protein adhesion than non-sulfated controls, indicating that the sulfation significantly reduced the thrombogenicity of the templates. Endothelial cell and SMC culture experiments showed no difference in attachment or morphology between the sulfated and non-sulfated templates. Endothelial cells and smooth muscle cells both proliferated well on the sulfated grafts while no non-sulfated control data was given. Immunohistochemistry and mRNA analysis of endothelial cell culture experiments indicated increasing activation of PECAM-1, CD146, and VE-C, indicating functionality of the endothelial cells, while SMC culture experiments showed increasing expression of smooth muscle myosin heavy chain, α-smooth muscle actin, and collagen type I, indicating SMC functionality (Liu et al. 2013). Unfortunately, no in vivo testing of these grafts was done.

3.2 Electrospinning

Electrospinning was first conceptualized in 1745 when Bose described the formation of aerosols from fluid droplets subject to high electric potentials (Bose 1745). The modern form of electrospinning was later developed in the 1930s when Anton Formhals filed a patent for the electrospinning of plastics. Eventually, electrospinning was applied in science in the 1990s by the Reneker group who formally investigated the process, processing conditions, fiber morphology and suggested possible applications (Doshi and Reneker 1995; Formhals 1934). The fabrication method of electrospinning involves taking a polymer solution, which can also contain drugs and other traditional additives for eventual release, and extruding that charged solution into an electric field. This field draws the solution towards a grounded mandrel, whipping it around into a thin micro- or nanofiber as the solvent evaporates. The fiber is deposited on a collection mandrel in a randomized fashion, where it interweaves with itself to form a fibrous material (Doshi and Reneker 1995; Huang et al. 2003; Yamashita 2007). By varying parameters such as flow rate, distance to the mandrel, and strength of the electric field, the fiber diameter and pore size of the electrospun material can be controlled (Greiner and Wendorff 2007; Reneker and Chun 1996). Electrospinning also allows fibers to be created with a core of one polymer, usually to provide tensile strength, and a coating of another, to typically control drug release or provide cell binding sites. Alternatively, electrospun materials can be coated with other materials after the electrospinning process via adsorption or covalent bonding. In one such effort, Zhu et al. electrospun a PCL fiber mesh using a mandrel rotating at a variety of speeds (700–2000 rpm). The resulting meshes were then dipped in a fibrinogen solution, and then a thrombin solution. The thrombin cleaved the fibrinogen into insoluble fibrin, which then aggregated in a coating on top of the PCL fibers. Scanning electron microscopy (SEM) images showed that the fibers became more aligned as the rotational speed of the mandrel increased. In vitro SMC testing showed that the cells had good adherence to the fibrin coating and, on the templates with aligned fibers, the smooth muscle cells oriented and stretched out along the long axis of the fibers. Comparison with non-fibrin-coated templates indicated that the fibrin promoted SMC proliferation (Zhu et al. 2010). These results show the benefits of aligned fiber templates in controlling SMC behavior as well as the benefits of fibrin coating in promoting SMC proliferation.

In a 2015 study, McKenna et al. electrospun tropoelastin, the monomeric elastin building block, into small-diameter vascular conduits. These conduits were then submerged in solutions of disuccinimidyl suberate (DSS), a cross-linker which creates amide bonds between the tropoelastin molecules. Mechanical testing of the grafts showed that their UTS was much lower than that of native carotid artery, with a lower elastic modulus, lower burst pressure, and lower percent elongation at break as well. In vitro testing showed endothelial cell adherence and proliferation on the graft (McKenna et al. 2012). These results show the benefits of electrospun elastin for cell attachment, but the mechanical testing results indicate that electrospun elastin by itself has insufficient strength to serve as a vascular graft.

In a more successful effort, Wong et al. electrospun aligned-fiber grafts from PU, a PU/collagen blend, a PU/elastin blend, and a PU/collagen/elastin blend. Grafts were then immersed in 1-ethyl-3-(3-dimethylaminopropyl)carbodiimide hydrochloride (EDC) and then Na_2HPO_4 to crosslink the proteins and thereby prevent their dissolution in aqueous environments. Mechanical testing showed that the PU/collagen and PU/collagen/elastin grafts were stiffer than the PU templates, while the PU/elastin graft was significantly more elastic. The PU/collagen and PU/collagen/elastin grafts enhanced the proliferation of smooth muscle cells seeded on the graft surface, while the PU/elastin graft had no change from the PU control. All three protein-blended composites showed greater smooth muscle actin staining intensity than the graft spun from just PU, indicating that both collagen and elastin helped the smooth muscle cells achieve a contractile phenotype (Wong et al. 2013). While the PU/elastin grafts were more rigid than native tissue, the results from this study demonstrated how the incorporation of elastin and collagen into the electrospinning process could help tune the final mechanical properties of the graft while enhancing cellular proliferation and function.

One of the greatest obstacles facing electrospun vascular grafts is ensuring adequate cellular infiltration throughout the structure. While mat porosity can be controlled during the electrospinning process, there is a tradeoff between increasing pore size and decreasing the mechanical strength of the construct. Also, because the nanofibers in an electrospun mat are deposited onto a flat surface, they become oriented parallel to that surface with randomized directions in a flat two-dimensional plane. The randomized packing makes it difficult to achieve total control over the interconnectivity of the pores, and the two-dimensional orientation of the fiber matrix does not provide clear fibrous pathways for cells to burrow into the structure (Leong et al. 2013; McClure et al. 2012; Selders et al. 2016; Wang et al. 2013). Some groups have developed methods using sacrificial fibers or other porogens to increase structure porosity. In a 2008 study, Baker et al. used a dual-electrospinning method with two spinnerets to create templates composed of PCL and PEO fibers. The quickly degrading PEO fibers were then removed by soaking the templates in an aqueous solution, which then opened up new, interconnected pores. In vitro experiments showed that mesenchymal stem cells (MSC) infiltrated more rapidly and easily into the constructs with these new pore spaces relative to controls spun from PCL (Baker et al. 2008). In a similar effort, Simonet et al. electrospun structures in a low-temperature, controlled-humidity environment in order to create ice crystals between the fibers that, when melted away, would leave void spaces (Simonet et al. 2007). While methods like these are successful at creating new pores, they often sacrifice the mechanical strength of the construct, and sometimes these pore spaces can be closed when the surrounding fibers shift and collapse them (Ekaputra et al. 2008; Lowery et al. 2010).

A more successful method of increasing graft porosity was developed in 2012 by McClure et al. Fibers were electrospun onto a hollow cylindrical mandrel with evenly spaced holes drilled through its wall. Air was forced into the cylinder and out through the holes during the electrospinning process, and this air pushed fibers away from these areas, creating zones of greater porosity. These zones successfully

increased permeability and cell penetration but initially compromised mechanical strength (McClure et al. 2012). In 2016, Selders et al. continued the work and showed that by varying the pore sizes of the mandrel, the velocity of the air flow, and the fiber size spun onto the mandrel, mats could be created with greater porosity while maintaining mechanical strength (Selders et al. 2016). While these air-impedance electrospun grafts have yet to be examined in vivo, these early data suggest that they will be more effective at eliciting cellular ingrowth than traditionally electrospun grafts.

Some groups have addressed the cellular ingrowth obstacle by abandoning the acellular approach and incorporating smooth muscle cells into the graft as it is electrospun. In a 2006 study, Stankus et al. electrosprayed a solution of smooth muscle cells in gelatin concurrently while electrospinning a PU graft, so that the smooth muscle cells would be incorporated throughout the resulting structure. No decrease in cell viability was seen after electrospinning. Perfusion culture of these grafts was shown to improve cell proliferation and integration. While mechanical testing showed the grafts to be both flexible and strong, the gelatin incorporation was shown to alter the fibrous structure and somewhat compromise the mechanical properties of the graft (Stankus et al. 2006). It should also be mentioned that this technique has many of the same drawbacks that cell-laden hydrogels have, including culture costs, potential genetic or epigenetic changes in the cells during culture, patient immunosuppression if donor cells are used, and time delays if autologous cells are used.

3.3 Sponges

Derived from their namesake, a sponge's reticular nature serves as a source of inspiration for biomimicry. Polymer sponges are often used to create microporous environments for cell attachment within a fibrous structure. These sponges can be created through freeze-drying a polymer solution or by removing the liquid from a crosslinked hydrogel structure (Aper et al. 2016; Liu et al. 2013).

Sugiura et al. investigated PLCL copolymer sponge scaffolds as small-diameter vascular grafts in the mouse model. Specifically, the grafts were constructed by pouring a 50:50 solution of PLCL into a glass tube. The glass tube was then subjected to freeze drying under a vacuum. Two separate groups with average pore sizes of 12.8 ± 1.85 μm and 28.5 ± 5.25 μm with an internal diameter of 0.6 mm were created (Sugiura et al. 2016). Afterwards, the grafts were reinforced via electrospinning a 40 μm thick layer of PCL onto the exterior of both groups. Grafts were then implanted at the infrarenal aorta of female mice for 8 weeks and evaluated. After 8 weeks, the group found that the grafts in all survived mice were patent with no aneurysmal dilatation. Two of the fifteen mice in the large pore group developed lower limb paralysis from acute thrombosis. Grafts were subject to CD31 staining for endothelial cells and α-smooth muscle actin (α-SMA) for smooth muscle cells. Both grafts were found to have a layer of endothelial cells followed by smooth muscle cells. Gene expression of PECAM and eNOS was also evaluated for the

quality of endothelialization. No statistical difference was found in this expression between the small and large diameter groups. Macrophage infiltration and M1 versus M2 phenotype were also evaluated via immunohistochemistry. Macrophage infiltration was found in both groups with no statistical difference in the ratio of M1 versus M2 between the groups (Sugiura et al. 2016). The authors hypothesized that the large pore group would promote cell infiltration, reduce inflammation, and promote greater vascular generation through the M2 macrophage. They commented that their large pore size group may not have had sufficiently large pores and that their range of pores within the large group contained too many small-diameter pores. The group concluded that their grafts showed well-organized neointimal formation and that no statistical difference could be seen between large and small-diameter pores.

4 Surface Modification

4.1 Methods of Surface Modification

Cells can only interact with a presented exterior surface of a material. Therefore, there is ample opportunity to exploit internal mechanical strength with exterior cell interactions. As a result, in addition to the wide variety of fabrication methods, many protocols have been developed to treat the surface of tissue interacting structures in order to bring about desired cellular responses such as cellular adhesion and proliferation. Many of these protocols are investigated in the context of a variety of tissue engineered template applications but have potential applications in vascular grafts.

4.1.1 Endothelial Cell Seeding

The endothelial layer serves as a defensive barrier against blood coagulation. Restoration of this barrier is paramount in a successful graft. Initial animal models showed excellent re-endothelialization results, but later studies revealed that humans do not readily regenerate an endothelial layer from trans-anastomotic cells or progenitor cells found in the blood (Berger et al. 1972; Clowes et al. 1986; Sauvage et al. 1974). The idea of seeding vascular grafts was first posed in 1978 by Malcom Herring and several investigators since have looked into methods of adding autologous endothelial cells prior to implantation (Herring et al. 1978). The entire process of endothelial cell seeding can be divided into two stages: cell acquisition and cell luminal surface application.

Endothelial cells can be autologously acquired through two techniques: cell scraping and cell digestion. In cell scraping, a vessel such as the great saphenous vein is mechanically scraped, yielding on average $<75\%$ of the available cells (Stanley et al. 1986). This process is limited to vessels large enough to be physically handled and thus are in limited supply. The other method is through enzymatic digestion by collagenase or trypsin. With this option, microvessels found in adipose

tissue become a readily available source of cells with an average harvest of 0.23–32.4 $\times$ 10^5 cells per gram of tissue (Tiwari et al. 2001).

After the acquisition of cells, there are three primary methods to apply these cells onto the graft luminal surfaces: gravitational, hydrostatic, and electrostatic. Furthermore, based on the degree of coverage, the terminology changes. For complete cell coverage, the term is cell sodding while partial coverage terminology is cell seeding. In cell seeding, the thought is that cells would multiply to confluence and reduce the amount of ex vivo culture time as well as cell harvesting quantity. In gravitational cell seeding, cells are placed within a graft and the graft optionally rotated. This method is usually paired with a "biological glue" such as fibrin to aid in cell adherence. Gravitation cell seeding techniques are typically hindered by a persistence of spheroid cell morphology resulting in high cell losses when implemented; furthermore, many of the biological glues used are prothrombogenic (Anderson et al. 1987; Kempczinski et al. 1987).

Hydrostatic cell seeding involves creating a pressure gradient either through internal pressure or external vacuum to adhere cells to the graft luminal surface. While this method quickly places cells in contact with a graft, the technique still has the same problems seen with gravitational cell seeding: cells have a spheroid cell morphology unless a significant (>2 h) incubation time is included (van Wachem et al. 1990). This incubation time poses a significant barrier to a viable commercial solution, as cells must be cultured in a hospital resulting in longer surgical times or multiple procedures.

In order to promote rapid cell adherence without thrombogenicity, the technique of electrostatic cell seeding was developed. In this method, the vascular graft serves as a dielectric material that can be temporarily charged while preserving a zero net charge. A positive charge can be placed on the interior surface of a graft which serves to attract endothelial cells which possess a negative charge. In 2001, Bowlin et al. explored the resilience of electrostatically seeded cells in an animal model. Autologous endothelial cells were harvested from canine jugular veins then labeled for in vivo tracking. Cells were then electrostatically seeded at +1.0 V onto 4 mm inner diameter, 6 cm long ePTFE grafts. The cells were seeded to complete nodal coverage density. This group has shown that adherence and morphological maturation of the endothelial cells can be obtained in 16 min. The grafts where implanted in canines using a femoral artery model for 1 week. After 1 week, there was 90.3 $\pm$ 14.3% coverage by endothelial cells compared to 6.82% $\pm$ 7.19% in the control group (Bowlin et al. 2001). This difference was significant ($p < 0.001$) and showed that electrostatic cell seeding could provide robust endothelial cell adherence in a reasonable turnaround time that the operating room would require.

4.1.2 Adsorption and Covalent Linking of Biomolecules

Another technique to change the surface chemistry of a biomaterial is affixing biomolecules directly onto the surface. A variety of biologically functional molecules can be immobilized to the surface of a material using several available techniques. The desired characteristics of the biomolecule delivery such as elution versus immobilization and bioactivity will determine setup complexity

and subsequent scalability. The core concept of adsorption is the adherence of a molecule to a surface though Van der Waals forces, hydrogen bonds, or ionic attraction. These molecules can be readily displaced, and proteins are prone to denaturation. Alternatively, covalent linking consists of the formation of covalent bonds between the material and molecule of interest. These setups require specific chemistry and are thus more complex to perform as well as scale up. This technique is advantageous in that molecules are tethered to the surface in order to maintain a constant concentration and, if done correctly, maintain bioactivity.

In a 2002 study, Zhu et al. immobilized gelatin, chitosan, and collagen onto a PCL film surface. PCL films were first treated with 1,6-hexanediamine-2-propanol to introduce free amino groups, then with glutaraldehyde to add longer linking groups. Solutions of gelatin, chitosan, or collagen were added for 24 h and then rinsed. Coupling of these biomacromolecules was confirmed using X-ray photoelectron spectroscopy. Their addition caused a significant decrease in water contact angle compared to non-treated PCL, indicating an increase in surface wettability, with little difference between the sample groups. Endothelial cell culture showed improved cell attachment and proliferation on all three sample groups as compared to non-treated PCL, with gelatin and collagen showing the greatest attachment, and gelatin and chitosan showing the greatest proliferation. Secretion of vWF was higher on all three sample groups relative to non-treated PCL, indicating more complete activation of optimal endothelial cell morphology (Zhu et al. 2002). The use of a PCL film, rather than a fibrous structure, creates a nonporous surface that is suboptimal for endothelial cell attachment; thus, it is logical that the adherence of fibrous proteins increased endothelial cell attachment. Nevertheless, this study demonstrates the benefits that such treatments could have on the luminal surface of a graft.

In a 2014 study by Pfieffer et al., grafts were created with an electrospun inner layer of either 2/1 ratio of PCL/PLA or 25/5/2 ratio of PCL/PLA/polyethylene glycol (PEG), surrounded by an electrospun PCL outer layer. In vitro testing showed improved endothelial cell adherence to PCL/PLA and PCL/PLA/PEG layers compared to the ePTFE controls. Conduits were then pre-treated with either blood, gelatin, or fibronectin by applying these respective additives to the graft lumen, relying on protein adsorption. The best endothelial cell adherence was observed on the fibronectin-treated surfaces of either PCL/PLA or PCL/PLA/PEG fibers, with 98% viability and widespread cobblestone morphology, whereas the fibronectin-treated ePTFE grafts only had a 55% viability. Fibronectin also significantly outperformed blood and gelatin for all three fiber types with regards to endothelial cell adherence and proliferation (Pfeiffer et al. 2014). These results thus demonstrate the benefits of both composite polymer grafts and fibronectin coating in establishing an endothelial cell layer on the graft lumen.

Similarly, Bastijanic et al. applied a fluorosurfactant (FSP) coating to the inside of ePTFE grafts to lower the surface tension of water and thus improve endothelial cell adhesion. First, the cell-adhesive peptides RGD and CRRETAWAC were complexed to a poly(vinyl amine) (PVAm) polymer backbone. Perflurocarbon chains were attached to this backbone, and then the complexed molecules were

dissolved in deionized water and applied to 4 mm inner diameter ePTFE grafts via a 24-h soak period. Some grafts were then incubated in 100% ethanol for 1–15 min and dried, as preparation for a hydrogel loading step. Water contact angle experiments showed that the polymer surface survived the ethanol incubation period, and X-ray photoelectron spectroscopy confirmed that the functional groups of the peptides were present as well. PEG hydrogels were also incorporated into these grafts.

First, the PEG was functionalized with either RGD groups or an enzyme-degradable VPMSMRGG peptide (VPM) sequence. Then, PEG solutions were applied to the extramural surface of the ePTFE grafts and crosslinked via ultraviolet (UV) light. Grafts were then frozen and lyophilized. X-ray photoelectron spectrography, SEM, and attenuated total refection-infrared spectroscopy indicated that the hydrogel penetrated at least somewhat into the luminal surface but primarily covered the outer adventitial surface. In vitro experimentation indicated a significant improvement in endothelial cell attachment with the presence of the CRETAWAC FSP coating over all other sample types, while the RGD FSP coated grafts with and without the PEG hydrogel had lower endothelial cell adherence, but still more than unmodified ePTFE. However, experiments had issues incorporating smooth muscle cells throughout the hydrogel, as it appeared that the ethanol used before the hydrogel incorporation process remained in the loaded templates and had a cytotoxic effect on seeded smooth muscle cells. Nevertheless, smooth muscle cells loaded onto non-graft functionalized PEG hydrogels showed enhanced spreading and interaction as compared to non-functionalized controls. These findings indicate that if the ethanol were to be eliminated from the hydrogel loading step, the hydrogel would likely enhance SMC infiltration into the grafts. Nevertheless, the data indicate that the functionalization of the ePTFE surface is helpful in establishing a luminal layer of native endothelial cells (Bastijanic et al. 2016).

4.1.3 Surface Degradation

A common strategy with surface modifications is to increase the material roughness to create more surface area and three-dimensional features for cell attachment. Furthermore, generation of new functional groups on the polymer surface also can concurrently increase cell attachment. These strategies can be achieved using an acidic or basic solution that degrades the surface of the polymer via hydrolysis. Ester bonds within polymers create hydroxyl and carboxylic acid groups when hydrolyzed to which cells can bind (Curtis et al. 1986; Ramsey et al. 1984). In a 2003 study, Yuan et al. developed a procedure to partially degrade PLA fibers using a concentrated NaOH basic solution. After 2.5 h of treatment, a rough topology was observed on the fibers but with no change in PLA crystallinity within the fibers. However, UTS and elongation at break did decrease significantly, indicating some compromise in the mechanical properties of the template (Yuan et al. 2003). In a similar study, Nam et al. treated films of PLA and PLGA with NaOH for a variety of incubation periods, up to 12 h. Increased hydrolysis time caused a decrease in water contact angle, indicating increased hydrophilicity of the polymer surface. X-ray photoelectron spectroscopy showed ether and carboxylic groups in the NaOH-treated films with respect to non-treated controls. In vitro

experimentation with hepatocytes revealed almost double the number of adhered cells on NaOH treated films than on the non-treated controls, with cell adhesion increasing with up to 1 h of NaOH treatment before dropping slightly with increased treatment time (Nam et al. 1999). While this study utilized hepatocytes, it is likely that similar results could be achieved with endothelial cells and smooth muscle cells.

The biggest drawback to using surface degradation to increase roughness and activate functional groups is the corresponding loss of mechanical properties. Because this procedure involves hydrolyzing the polymer backbone, care must be taken to only expose the surface of the construct to the degrading solution. If the load-bearing elements are also degraded, then the structure will not be able to withstand the mechanical forces necessary to function as a vascular graft.

4.1.4 Surface Micropatterning

Surface area and geometry are paramount variables for subsequent cell behavior. Evidence collected over the past 20 years by a variety of groups has shown that the presence of micro- and nano-grooves and channels aids endothelial cell attachment and migration under flow conditions (Biela et al. 2009; Li et al. 2001; Uttayarat et al. 2008; Uttayarat et al. 2005; Zorlutuna et al. 2009). Three main categories of micropatterning methods are photolithography, electron beam lithography, and soft lithography. Photolithography is accomplished by exposing a light-sensitive polymer to UV light through patterned gaps in a non-light-sensitive blocking sheet. Depending on the characteristics of the light-sensitive polymer, the UV light will cause it to polymerize, become crosslinked, or to degrade. Then, the polymer is treated to chemically remove the excess polymer, leaving a patterned layer. The resolution of patterning is a function of the wavelength of the light used. In electron beam lithography, a beam of high-energy electrons is raster scanned across a layer of light-sensitive polymer, exposing the material underneath. Because the resolution of this method is a function of the diffraction limit of electrons, smaller (submicron) patterns can be created (Biswas et al. 2012). Both photolithography and electron beam lithography are high-cost and low-throughput methods, complicating the scale-up of these technologies. In contrast, soft lithography, which makes use of elastomers to emboss, print, and mold patterns onto surfaces, is lower cost and allows for a higher throughput at the expense of reproducibility.

Miller et al. used soft lithography to create nano-patterned PLGA films for vascular grafts. First, a PLGA film was treated with NaOH to create rough surfaces with micro- and nano-features based on NaOH treatment time. A silicone elastomer was then poured on top of these surfaces and cured to create a negative cast of the surface structure. PLGA was then poured on top of these elastomer molds and allowed to solidify. In this way, the rough topography created by the NaOH treatment was transferred to new films without the chemical modifications that NaOH makes to the polymer structure. Atomic force microscopy (AFM) data and SEM images confirmed the transfer of topographical features from the NaOH treated PLGA to the elastomer, to the final PLGA membrane. While adhesion and proliferation decreased on NaOH-treated PLGA relative to untreated PLGA, endothelial cells adhered and proliferated significantly better on nano-structured cast

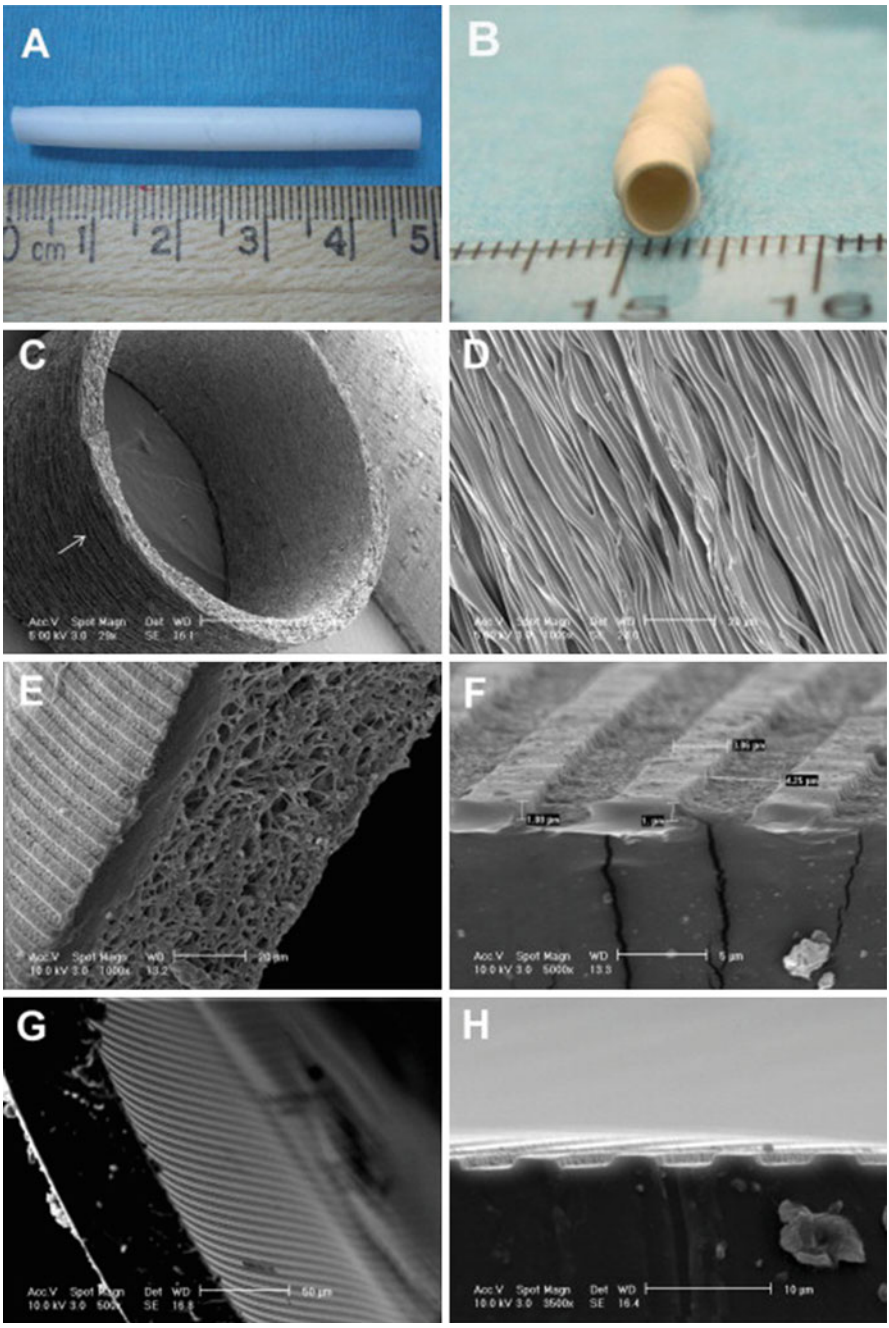

Fig. 12 Small diameter PU grafts fabricated by electrospinning resulting in (**a**) a graft length of 48 mm and (**b**) a graft diameter of 4 mm. (**c**, **d**) SEM images of electrospun graft showing the arrangement of microfibers that wind circumferentially (arrow) around the graft. (**d**) Individual

PLGA. Smooth muscle cells adhered and proliferated better on both NaOH-treated and cast PLGA films relative to untreated PLGA control films (Miller et al. 2004).

In a more recent study, Uttayarat et al. created 4 mm diameter PU grafts with microgrooves on their luminal surfaces to promote endothelial cell attachment (Fig. 12). A micropatterned PDMS sheet with microgrooves (3.6 μm channel × 3.3 μm ridge × 1 μm depth) was wrapped around a cylindrical mandrel, and then a PU solution was slowly poured over the mandrel as it rotated in a procedure known as spin casting. A high-intensity halogen lamp was used to cure the PU around the mandrel, forming a micropatterned cylindrical tube. PU nanofibers were then electrospun onto the outside of the grafts. SEM images confirmed the transfer of grooves to the luminal surface of the PU. Mechanical testing confirmed that the elastic modulus of this graft was close to that of native rabbit aorta tissue. Ultimate tensile strength and burst strength were not tested. In vitro evaluations with endothelial cells showed that the unidirectional microgrooves provided contact guidance to the cells, causing them to elongate and align parallel to the microgrooves. However, this alignment was no greater on the microgrooves than on aligned electrospun fibers (Uttayarat et al. 2010).

Relative to other graft fabrication methods, micropatterned films have significant drawbacks. Their lack of pores presents an obvious barrier to tissue ingrowth and cellular communication between the endothelial cell and SMC layers. Additionally, there is little data on the mechanical properties of these films after in vivo degradation. As such, it is unclear whether grafts constructed of micro- and nano-patterned films will remain patent long-term. While the micropatterning technologies discussed above allow for greater control of surface topography, the findings of Uttayarat et al. show that it is unclear whether this control provides any significant benefit over the surface topography achieved by electrospinning.

4.1.5 Co-electrospinning and Coaxial Electrospinning

Co-electrospinning and coaxial electrospinning are methods of surface modification unique to electrospinning alone. These techniques have the advantage of concurrent surface modification with the primary structure, thus eliminating the need for a post-processing modification step.

In co-electrospinning, biomolecules are placed in the polymer solution prior to electrospinning and then become incorporated into the fibers during the electrospinning process. This process is useful both for functionalizing the fiber surface and for establishing a controlled release of the biomolecules. In a 2005 study by

Fig. 12 (continued) microfibers taken from the graft exterior in (**c**) are shown to be tightly packed and aligned. (**e**, **f**) SEM images of hybrid graft consisting of microgrooves on the lumen and mesh of microfibers on the exterior. (**g**, **h**) SEM images show a PU graft generated by spin casting alone. The ridge width, channel width and channel depth were 3.6 ± 0.2, 3.9 ± 0.1, and 0.9 ± 0.03 μm, respectively, in (**f**) and (**h**). (Reprinted from Acta biomaterialia, 6:4229-4237, Uttayarat et al., Micropatterning of three-dimensional electrospun polyurethane vascular grafts, Copyright (2010) with permission from Elsevier)

Kwon et al., PLCL was co-electrospun with 5%, 10%, 30%, and 50% collagen I (for surface functionalization) or 1%, 5%, and 10% tributylamine-heparin salt (for controlled release). For further comparison, a subset of PLCL fabrics was coated with fibronectin. SEM images showed the collagen-containing fibers had lower diameters than pure PLCL controls, and mechanical testing showed that the tensile strength of the templates decreased with increasing concentration of collagen. The heparin-loaded templates were not tested. Endothelial cells seeded on the templates showed higher elongation and spreading on 5% and 10% collagen-blended templates, while endothelial cells on 30% and 50% collagen-blended templates had less spreading and were more rounded. The authors attribute this suboptimal morphology on the higher collagen content templates to the higher degree of fiber swelling and corresponding template shrinkage when placed in aqueous environments. 5% and 10% collagen-loaded templates and the fibronectin-treated templates had significantly higher endothelial cell proliferation than the untreated PLCL control, while 30% and 50% collagen-loaded templates had significantly lower numbers of adhered endothelial cells than untreated PLCL. Heparin release experiments showed an initial 12-h burst release proportional to the loading amount, followed by a 4-week consistent release period. Predictably, the more heparin loaded into the construct, the larger cumulative release of heparin from the construct over the 4-week period. This release profile suggests that some of the heparin was present on the fiber surfaces and solubilized quickly once placed in liquid, thus creating a burst release. The following period of controlled release was likely a result of slow PLCL hydrolytic degradation, freeing up small deposits of heparin present throughout the fiber interior. This account was supported by SEM images taken at the end of the 4-week release period, which showed disconnected and thinned fibers consistent with slow PLCL degradation. Toluidine blue imaging showed heparin present at the surface of fibers before the release period, further validating this release theory (Kwon and Matsuda 2005).

Coaxial electrospinning, a procedure in which one nozzle is placed inside another and solution is forced out of both during the electrospinning process, allows the creation of fibers with a distinct core/shell morphology. A core load-bearing polymer can be surrounded by a biopolymer shell to create surface-functionalized fibers. Alternatively, a shell of load-bearing polymer can surround a drug-containing core whose release is delayed and controlled by the degradation of the polymer shell. In a recent 2017 study, Hu et al. used coaxial electrospinning to create heparin- and vascular endothelial growth factor (VEGF)-loaded fibers. This procedure was used to encapsulate VEGF and the anticoagulant heparin in a core surrounded by collagen/elastin/PLCL and pure PLCL shells. A sustained release of heparin and VEGF was observed over a 4-week release period, with a significant burst release of heparin in the first 24 h. Endothelial cells cultured on VEGF-loaded templates had significantly better attachment and proliferation as compared to ePTFE and non-loaded PLA/PCL fibers. Grafts were implanted into rabbit aortas for 28 days and showed better patency than ePTFE controls, and post-explantation analysis showed less thrombus formation than ePTFE (Hu et al. 2017).

In a similar study, Yin et al. used coaxial electrospinning to encapsulate a heparin core within a collagen/chitosan/PLCL shell for controlled release from

small-diameter grafts. Mechanical testing showed the higher the PLCL content of the shell, the greater the peak stress and strain at break, with 50% or higher PLCL content creating grafts that were significantly stronger than native artery. Heparin incorporation did not have a significant effect on graft strength. The incorporation of 5% heparin increased graft compliance relative to non-loaded control, but concentrations above the 5% level decreased compliance significantly. Most graft formulations tested achieved higher burst pressures than those of native saphenous vein. A heparin encapsulation efficiency of at least 70% was achieved in all but one formulation. Release experiments showed all formulations having a controlled release period of at least 45 days following an initial burst release. Platelet adhesion testing showed significantly less platelet adhesion as compared to a pure electrospun PLCL control. Endothelial cell culture testing showed that the template with the highest initial burst release of heparin had lower endothelial cell proliferation than the best performing non-control samples, but all other heparin-releasing templates showed no difference from each other or non-heparin PLCL controls. SEMs showed endothelial cell spreading on all template surfaces. These data indicate that while high heparin concentrations can impede endothelial cell behavior, a controlled release of heparin can be achieved which reduces platelet adhesion without impeding endothelial cell growth (Yin et al. 2017).

4.2 Materials of Surface Modification

In the search for the ideal biomaterial, researchers have come to realize that there is no universal material for all applications, and that the myth of the ideal inert biomaterial is just that. Therefore, researchers have investigated artificially recreating both the chemical as well as mechanical signals found in the in vivo environment. Most of the biomolecules that make up a cell's environment are expensive to harvest, and in most applications lack the necessary mechanical properties that modern techniques afford in implementing these materials. Thus, many researchers turn to modifying the surface of synthetic materials with biomolecules using the aforementioned techniques, thereby blending the ideal mechanical properties with the ideal cellular responses.

Initial surface modifications began in the operating room. Due to issues of blood leakage in early porous grafts, especially with heparinized patients, surgeons would implement various techniques of pre-clotting their grafts in the patient's blood (Yates et al. 1978). Alternatives soon came on the market to pre-coat vascular grafts with molecules such as albumin, heparin, collagen, and gelatin. In addition to solving the issue of leaking, preconditioning the material surface influences the cellular response to the vascular graft.

4.2.1 Albumin

Albumin is the most common protein in human blood plasma. It is constitutively produced in the liver and serves to transport molecules such as hormones and fatty acids. It has a serum half-life of approximately 20 days and a molecular mass of

66.5 kDa (Peters Jr 1995). In addition, albumin is responsible for maintaining oncotic pressure in the body.

Kottke-Marchant et al. studied the in vitro blood compatibility of an albumin coating on Dacron vascular grafts. Albumin-coated Dacron compared to Dacron grafts were evaluated for platelet activation, fibrin formation, and leukocyte interaction at up to 3 h. Platelet activation via release of platelet factor 4 and β-thromboglobulin was found to be significantly less in the albumin coated grafts, and they also had less coagulation activation via fibrinopeptide A formation (Kottke-Marchant et al. 1989). SEM imaging showed that Dacron alone had more adherent leukocytes and platelets than did the albumin coated Dacron grafts. This study showed that in addition to reducing blood leakage, molecules such as albumin can precondition the material surface to change the cellular response.

In addition, Kangac et al. studied the effects of coating knitted Dacron grafts with albumin and evaluating for tissue ingrowth amongst other parameters. Canines were subject to thoracoabdominal aortic resection and had an 8 mm internal diameter, 30 cm long graft implanted. Two groups consisting of carbodiimide-cross-linked human albumin bound onto the surface of knit Dacron grafts were compared to knit Dacron grafts pre-clotted with whole blood. Grafts were evaluated at 1, 4, 10, and 20 weeks. All evaluated grafts were patent, and there was no significant difference in the evaluation of tissue incorporation. The albumin-coated grafts had inner capsules comprised of myofibroblasts, collagen, and endothelial cells that had a thickness 20% less than the Dacron control (Kangac et al. 1997). This difference of 0.045 mm was significant and may indicate a lesser propensity for intimal hyperplasia.

4.2.2 Collagen

Type I collagen is a major extracellular matrix component of the vascular system and is deposited in the vascular tissue by fibroblasts and smooth muscle cells. It is characterized by a triple-stranded helix with each chain composed of the amino acid sequence Gly-X-Y where X is typically a proline and Y is frequently a hydroxyproline (Rhodes and Simons 2007). Structurally, it is the primary load-bearing component of the vasculature and also provides integrin binding sites that enable cell attachment and movement within the extracellular matrix (Boland et al. 2004; Caves et al. 2010; Kumar et al. 2013). These integrin binding domains facilitate cell adhesion and are characterized by RGD (Arg-Gly-Asp) sequences (Ruoslahti 1996). One drawback to using collagen in vascular applications is that it is highly thrombogenic. In the natural vasculature, collagen is usually only exposed directly to the blood in the event of an injury, when it causes platelets to attach and activate (Wise et al. 2011). To address this problem, a variety of strategies have been developed, including pre-seeding collagen templates with endothelial cells or using an acid-soluble collagen I variant with higher clot resistance than ePTFE (Boccafoschi et al. 2005; Tillman et al. 2009). Surprisingly, another issue with collagen-based vascular grafts has been their structural integrity. One of the first serious attempts at a tissue-engineered graft, created by Weinberg and Bell in 1986, involved seeding gels of collagen I with bovine endothelial cells, smooth muscle cells, and fibroblasts to create layers similar to the natural intima,

media, and adventitia of native vascular tissue (Weinberg and Bell 1986). Their original model constructed with one mesh has a burst strength of 40–70 mmHg, failing via delaminating and tearing. A further model consisted of three layers of collagen lattice that alternated with two Dacron meshes. This graft had a burst strength of 120–180 mmHg and failed by a pinhole leak. The mode of failure with these grafts resided with the collagen lattice. In a final effort, the authors optimized the collagen deposition and cross-linking to produce grafts that had a burst strength of 323 ± 78 mmHg. While a significant improvement, these grafts had a burst pressure an order of magnitude less than native human vascular burst pressure, which presents a significant barrier to in vivo applications.

More recent attempts have involved combining collagen with one or more other polymeric materials. In a 2015 study, Koens et al. created three-layered 4 mm inner diameter vascular conduits by taking elastin and type I collagen fibers purified from equine ligament and bovine Achilles tendon, respectively, and depositing them via a molding, freezing, and freeze-drying method. An elastin layer was first deposited, followed by two subsequent collagen layers, and then the grafts were crosslinked with EDC and N-hydroxysulfosuccinimide (NHS) in the presence of heparin so as to deposit heparin onto the graft surface. The materials were then grafted into porcine bilateral iliac arteries and left for a period of 7 or 28 days. Duplex scanning showed all grafts remained patent after 7 days, with turbulence observed at the anastomoses. After 28 days, though, all the experimental grafts were completely occluded, as opposed to only 1 of 4 ePTFE control grafts. Explantation revealed dislodged elastin fibers, with a fibrin layer forming between the elastin layer and the first collagen I layer, and alizarin red staining revealed significant calcification of the graft. The authors postulate that the large surface area of the fibers coupled with blood shear stress through the porous elastin layer contributed to the subsequent occlusion (Koens et al. 2015). Additionally, the fact that a significant amount of blood flow penetrated the elastin layer and came in direct contact with the first collagen I layer likely exposed it to the thrombogenic properties of the collagen. The information presented in this study represents a cautionary tale about the use of porous surfaces in vascular grafts. While some porosity is necessary to allow endothelial cell adhesion and tissue penetration throughout the graft, too much porosity creates dangerous fluid shear through the fibers that, along with other factors, can contribute to thrombotic occlusion of the graft. One potential improvement would be to compact this inner layer somewhat, so that a smoother inner surface is created that still has enough porosity to allow for endothelial cell attachment and proliferation.

Some researchers have postulated that the poor mechanical stability of vascular grafts made from collagen gels is due to the fact that smooth muscle cells seeded on their surfaces tend to take on longitudinal orientations, rather than the circumferential orientation found in native vascular tissue (Kakisis et al. 2005). This orientation can be addressed by the use of a pulsatile flow bioreactor which provides the cyclic stretch experienced by smooth muscle cells in native arteries within the body (Sarkar et al. 2007). In another 2015 study, Ahn et al. created vascular grafts by electrospinning a 1:1 blend of PCL and calf skin collagen I onto a

4.75 mm diameter cylindrical mandrel. This sheet was then crosslinked using 2.5% glutaraldehyde vapor and combined with three layers of ovine vascular smooth muscle cells wrapped around the outside of the graft. Control grafts were prepared by seeding trypsin-dissociated individual vascular smooth muscle cells on the outside of identical electrospun constructs. These grafts were then loaded into a pulsatile perfusion bioreactor which applied physiological stretch, pressure, and flow (of culture medium, not blood).

After a period of 5 days, the grafts were removed, fixed, and examined. Immunofluorescent staining showed that the grafts surrounded by confluent layers of smooth muscle cells showed higher expression of cell-to-cell junction proteins and contractile proteins than the SMC-seeded grafts. The cell sheets maintained structural integrity with their electrospun templates throughout the pulsatile flow culture period, with greater migration into the structure than non-pulsatile culture controls. Mechanical testing before and after the 5-day culture period indicated that the pulsatile culture period significantly increased the tensile strength and elongation at break of the cell sheet-wrapped structures, and decreased the elastic modulus, thus allowing the graft to flex further with the flow. Additionally, this testing showed that the structures surrounded by a cell sheet had significantly greater tensile strength, lower elastic modulus, and greater elongation at break than the non-wrapped template controls after the pulsatile culture period, indicating that the SMC layer mediated the structural changes undergone by the graft during the culture period (Ahn et al. 2015). While this study demonstrates the benefit of incorporating a SMC layer into the outside of a vascular graft, as well as the use of collagen I to enhance the binding and infiltration of this cell layer into the graft, it fails to address potential thrombogenicity concerns arising from the bloodstream directly contacting the collagen I within the graft.

Another method of improving the mechanical properties of natural polymers such as collagen or elastin is to use a crosslinker. Examples include UV radiation, genipen, NHS, EDC, and glutaraldehyde, among others (Drury and Mooney 2003; Jeong et al. 2007). Crosslinking with UV radiation is advantageous because there is no risk of the grafts leaching potentially harmful chemical crosslinkers after implantation, and UV radiation binds the aromatic tyrosine and phenylalanine residues of the collagen, rather than carboxylate anions, thereby preserving biologically functional binding sites (Davidenko et al. 2016). However, it may be difficult for UV radiation to penetrate deeply into a polymeric graft, thus limiting the degree of crosslinking.

A 2013 study by Chan et al. showed that crosslinking of collagen templates enhances the stability of adhered endothelial cell layers, thus improving both the mechanical stability and the ability of the grafts to resist thrombotic occlusion. Microvessel-mimicking collagen I gels were formed around 120 and 140 μm diameter needles, crosslinked with varying amounts of either genipen or EDC, then flushed with PBS to remove any residual crosslinker. The graft interiors were then perfused with a suspension of endothelial cells, which adhered and proliferated to form a confluent layer. Elastic moduli of the grafts increased with increasing concentration of both EDC and genipen during crosslinking, indicating that both

crosslinkers significantly increased graft stiffness. However, the permeability of the graft walls was unchanged by either crosslinking process, indicating that the wall porosity was unchanged. Perfusion of these grafts at low shear stresses showed that the endothelial cell layers on non-crosslinked templates tended to delaminate from the template and block flow through the graft, while the endothelial cell layers on both EDC and genipen-crosslinked templates remained fully attached and functional. Grafts were then perfused in a condition mimicking low transmural pressure, another condition which often destabilizes vessels. As was seen in the low-shear condition, endothelial cell layers dislodged from non-crosslinked templates, while those on EDC and genipen-crosslinked templates remained stable and functional (Chan et al. 2014). These results demonstrate the benefits of crosslinking collagen templates on overall graft functionality.

4.2.3 Elastin

Elastin comprises around 50% of the dry weight of arterial walls, and its distensible nature imparts the elasticity that allows these walls to flex outward as blood is pumped through them (Patel et al. 2006). It is formed by crosslinking its precursor molecule, tropoelastin, via the enzyme lysyl oxidase. Elastin's structure consists of two small segments alternating along a polypeptide chain (Rhodes and Simons 2007). One segment is hydrophobic and gives rise to elastin's elastic properties. The other segment is alpha-helix rich and is the site of where crosslinking occurs. Elastin has been shown to prevent the excess migration and proliferation of smooth muscle cells that is a defining characteristic of intimal hyperplasia (Patel et al. 2006). Elastin is often used in composite grafts along with a more rigid polymer to control the flexibility and compliance of the graft. In a 2008 study, Smith et al. fabricated 1.5 mm inner diameter tubes of electrospun PDO/elastin solutions. First, separate solutions of 60 mg/mL PDO and 200 mg/mL bovine elastin in 1, 1, 1-3, 3, 3-hexafluoro-2-propanol (HFP) were blended at a 70:30 volumetric ratio. The resulting blend was then electrospun onto a 1.5 mm diameter cylindrical mandrel. Halfway through the electrospinning process, a PDO suture was wound around the tube in a controlled manner to increase the mechanical integrity of the graft. A subset of tubes was created with two sutures applied between layers, one wrapping in a right-handed helix around the tube while the other wrapped in a left-handed helix. Another subset of tubes was fabricated without sutures or with one suture, or with only one layer. The tubes were soaked in EDC to crosslink the elastin as previous work has shown un-crosslinked elastin will elute out from hydrated electrospun templates, and then mechanically tested. The double-layered two-suture tube had the highest burst strength and lowest compliance, with crosslinking decreasing compliance. In general, the single-layered tube and the double-layered tube without suture best matched the compliance of native arteries and veins, but the burst strengths of all constructs tested were below those of the native tissues and the ePTFE control. Thus, while the results of this study indicate that PDO/elastin composite grafts match the compliance of native arteries, even the incorporation of a suture reinforcement does not give them the requisite burst strength (Smith et al. 2008).

4.2.4 Fibrin

Fibrin is a natural blood clotting protein used by the body to create a thrombus in the event of injury. Soluble fibrinogen, the precursor protein, circulates through the bloodstream until it reaches the site of an injury, where it is cleaved by the enzyme thrombin and forms aggregates of fibrous fibrin protein. Under trade names such as Evicel and TISSEEL, fibrin is used in the clinic as a tissue sealant and hemostatic agent. In a 2001 study, Grassl et al. investigated the use of fibrin in mimicking the media layer of a native vessel. Smooth muscle cells were entrapped within a solution of fibrinogen and thrombin, which was gelled into hemispherical constructs. Similar SMC-containing hemispheres were constructed of collagen I. The smooth muscle cells contained in the fibrin constructs produced higher levels of soluble and insoluble hydroxyproline than those entrapped in the collagen I gels, indicating increased production of new collagen (Grassl et al. 2002). It should be noted that this study made no attempt to mimic the structure or load-bearing function of the media layer, so while its results suggest that the presence of fibrin would be helpful in stimulating SMC remodeling of this layer, these findings do not indicate whether a graft utilizing a pure fibrin hydrogel in the media layer would succeed in vivo.

More recent work has succeeded in developing mechanically stable fibrin tubes. In a 2016 study by Aper et al., fibrinogen precipitated from human blood was clotted via thrombin into fibrinogen inside a high speed rotational mold. The centrifugal effect of the rotating cylinder forced the precipitating fibrin to the walls, forming tubes with inner diameters between 5.3 and 6 mm. During the centrifugation process, the liquid was forced out. This centrifugal spinning process compacted the fibrin, increasing the covalent crosslinking of the fibers as they formed and improving the overall mechanical strength of the tube. Some tubes were formed with fibrinogen solution containing fibrin stabilizing factor (factor XIII), while others contained both factor XIII and smooth muscle cells in the solution during spinning. Those tubes whose matrices were formed with smooth muscle cells inside had a layer of endothelial cells sprayed on the luminal surface after initial formation of the tube, which was then spun for 20 more minutes to promote endothelial cell attachment. Mechanical testing showed the tubes increased in strength with higher spinning rates, up to 15,000 rpm, and the addition of clotting factor XIII and smooth muscle cells to the initial fibrinogen solution and subsequent coverage with an endothelial cell luminal layer increased the tensile and burst strength of the tubes while decreasing their elastic moduli. Grafts constructed with factor XIII, smooth muscle cells, and endothelial cells were implanted into ovine carotid arteries and removed after either 1 or 6 months. Explantation after 1 month revealed only one out of three grafts were patent, with the other two occluded. The patent graft showed an increase in wall thickness characteristic of intimal hyperplasia, but immunofluorescent staining revealed only a few vWF-positive cells remained on the luminal side of the graft, indicating that most of the endothelial cells had been sheared off the surface. Explantation after 6 months revealed two out of three patent grafts, with a confluent layer of vWF-positive cells on the inside of the graft. This indicates that while the original endothelial cell layer sheared off, more endothelial cells arrived either through the blood or from the anastomoses to re-establish this confluent layer.

A large presence of α-SMA positive cells was seen in the neo-media of grafts at both 1 and 6 months, and histological staining showed that after 6 months, the fibrin grafts were remodeled with newly deposited collagen I. Post-explantation mechanical testing showed the fibrin grafts had lower tensile strength, burst strength, and elastic modulus than native ovine carotid artery, although evidently these grafts were strong enough for at least some of them to remain patent over the 6-month period (Aper et al. 2016). These results demonstrate the potential of fibrin-based vascular grafts but clearly more refinement must be done before they are considered a viable graft for use in humans.

Moving towards that goal, Syedain et al. has had some success with developing "off the shelf" arteriovenous grafts (AVG) in both sheep and baboons (Syedain et al. 2014, 2016, 2017). Their grafts were constructed by suspending human dermal fibroblasts (hDFs) in a fibrin gel and thrombin mixture. The suspension was injected into a tubular mold and maintained for a 2-week maturation period. The grafts were then transferred to a pulsatile flow bioreactor for an additional 3 weeks. Grafts were 4–6 mm in inner diameter and 12–15 cm long. After maturation the grafts were decellularized and stored for up to 12 months for implantation. Initial studies in sheep up to 6-months showed a population of appropriate cells without a prolonged inflammatory period and growth as the young lambs matured. Upon explantation, the synthetic polymer was not present, removing a potential source of chronic inflammation.

In their latest study, grafts were implanted into baboons between the axillary artery and the cephalic or brachial vein. Grafts were evaluated at regular time points between 1 and 6 months for mechanical properties, composition, histology, and immunohistochemistry. Initial mechanical properties of the grafts were found to be wall thickness of 0.48 ± 0.05 mm, UTS was 3.8 ± 0.7 MPa, circumferential modulus was 10.2 ± 2.2 MPa, burst pressure was 3164 ± 342 mmHg (99.8% of the reported value for the human internal mammary artery), and suture retention was 199 ± 56 gram-force (144% of the value reported for the native internal mammary artery). Their initial implantation protocol had to be adjusted to add the anticoagulant clopidogrel due to issues of venospasms resulting in thrombosis.

At 3 months, the primary patency rates were 83% (5 of 6) and at 6 months 60% (3 of 5). The authors commented that Dehl et al. performed a directly comparable AVG study in baboons with a 3- and 6-month patency rate of 83% and 100%, respectively, with no rapid initial failure due to clotting (Dahl et al. 2011). They conclude that some of the early issues they experienced were due to model development. One graft experienced rupture which the authors contribute to manufacturing defect. At 6 months postimplantation, the explanted grafts had a burst pressure of on average 156% of preimplanted values, indicating cellular ingrowth augmenting the mechanical properties. Grafts at 3 and 6 months stained positive for elongated cells with circumferential orientation (most of these in a region adjacent to the luminal surface also stained positive for α-SMA indicating smooth musculature phenotype), abundant collagen, minimal mature elastin, no calcification, and complete CD31 positive staining indicating endothelialization of the proximal and distal ends of a subset of the grafts.

Immunocompatibility analysis via IgG, IgM, and IgE showed no increase at all time points except a transient increase in IgE for one baboon. The authors believed this to be a type 1 hypersensitivity reaction due to incomplete removal of antigens. Overall, this study demonstrated a viable off the shelf, acellular solution to small-diameter vascular grafts. Nevertheless, issues with the baboon model and its external validity to human physiology are yet to be understood.

4.2.5 Heparin

Heparin is a negatively charged glycosaminoglycan with repeating disaccharide units. In vivo and clinically, heparin is used as an anticoagulant whose mechanism of action works through binding to activate the enzyme inhibitor antithrombin III (AT). AT in its activated form goes on to inactivate thrombin and factor Xa, two molecules involved in the coagulation cascade. Heparin is used to coat vascular grafts amongst other uses under the trade name CARMEDA® Bioactive Surface as an example.

There are three categories of methods for incorporating heparin into a graft: adsorption, electrostatic deposition, and covalent bonding (Hoshi et al. 2013). Adsorbed heparin is subsequently released as a burst in vivo with short-lived therapeutic effects and can result in the idiopathic pathology of heparin-induced thrombocytopenia, or HIT syndrome (Hoshi et al. 2013). Electrostatic deposition takes advantage of heparin's significant negative charge. A positive charge can be induced onto a graft to attract heparin to the graft. Post adherence, this method has the same issues as traditional adsorption with burst release. The last available option is covalent bonding. This method requires specific chemistry to immobilize heparin to a material. It was quickly discovered that heparin needs to be bound to a vascular graft in a way that preserve its tertiary and quaternary structure (Hoshi et al. 2013). Heparin's mechanism of action is dependent on its negative charge as well as its tertiary and quaternary structure to be biologically active. If covalently bound in such a way that the higher structure is lost, then the deposition becomes ineffective.

Hoshi et al. studied the effects of covalently bound heparin onto ePTFE vascular grafts. Specifically, the group bound heparin to aminated poly(1,8-octanediol-*co*-citrate) (POC) via its carboxyl functional groups onto POC-modified ePTFE grafts. The authors confirmed that this method of immobilization resulted in bioactive heparin for at least 1 month in in vitro physiologic conditions. Once the bioactivity was confirmed through whole blood clotting assays, the modified graft was evaluated for its interactions with isolated human endothelial cells, endothelial progenitor cells, and smooth muscle cells. Endothelial progenitor cells were studied through blood outgrowth endothelial cells (BOECs). These cells arise from bone marrow derived, circulating endothelial progenitor cells, and play a role in vasculogenesis.

Both cell lines of human umbilical vein endothelial cells (HUVECs) and BOECs showed viability and proliferation with no significant difference between the POC-Heparin group, POC, and tissue culture polystyrene groups (Hoshi et al. 2013). In addition, the HUVECs and BOECs stained positive for vWF and E-Cadherin as well

as produced nitric oxide which was confirmed by a fluorescent probe 5,6-diaminofluorescein diacetate assay. These results indicate that POC-heparin does not deter endothelial growth when compared with TCP controls. Human aortic smooth muscle cells (HASMC) showed a greater expression of α-actin on POC and POC-heparin compared to TCP (Hoshi et al. 2013). This protein is typically associated with the contractile smooth muscle phenotype as opposed to the proliferative phenotype. This is advantageous for a functional vascular graft and to avoid smooth muscle hyperplasia. Furthermore, the surface density of HASMC cells was significantly less in the POC-heparin and POC groups compared to TCP. This finding further reinforces that the smooth muscle cells were adopting a contractile phenotype rather than a proliferative one. These studies suggest that vascular grafts covalently modified with heparin can reduce thrombosis as well as smooth muscle hyperplasia, both of which are the two most significant causes of failure in vascular grafts.

5 Conclusions

With the rate of cardiovascular disease projected to rise over the next 10 years, the lack of a clinically available synthetic small-diameter vascular graft presents an urgent need. The research discussed throughout this chapter describes a variety of material choices, fabrication methods, and surface treatments which provide promising avenues towards the creation of novel vascular grafts. Such grafts should have burst pressures and UTS in excess of native vascular tissue, while closely matching the elasticity and compliance of that tissue. Porosity and pore interconnectivity should be tailored to allow for cellular ingrowth without creating high-shear flow conditions on the luminal surface of the graft. Cellular adhesion and proliferation can also be promoted via surface treatment and biopolymer conjugation. It is likely that the ultimate success of small-diameter vascular grafts will depend on the ability to mimic native artery tissue as closely as possible.

References

Abbott WM, Megerman J, Hasson JE, L'Italien G, Warnock DF (1987) Effect of compliance mismatch on vascular graft patency. J Vasc Surg 5:376–382

Ahn H et al (2015) Engineered small diameter vascular grafts by combining cell sheet engineering and electrospinning technology. Acta Biomater 16:14–22

Akbari M et al (2016) Textile technologies and tissue engineering: a path toward organ weaving. Adv Healthc Mater 5:751–766. https://doi.org/10.1002/adhm.201500517

Alexander JH, Smith PK (2016) Coronary-artery bypass grafting. N Engl J Med 375:e22. https://doi.org/10.1056/NEJMc1608042

Anderson JS, Price TM, Hanson SR, Harker LA (1987) In vitro endothelialization of small-caliber vascular grafts. Surgery 101:577–586

Aper T, Wilhelmi M, Gebhardt C, Hoeffler K, Benecke N, Hilfiker A, Haverich A (2016) Novel method for the generation of tissue-engineered vascular grafts based on a highly compacted fibrin matrix. Acta Biomater 29:21–32

Bagnasco DS, Ballarin FM, Cymberknop LJ, Balay G, Negreira C, Abraham GA, Armentano RL (2014) Elasticity assessment of electrospun nanofibrous vascular grafts: a comparison with femoral ovine arteries. Mater Sci Eng C Mater Biol Appl 45:446–454. https://doi.org/10.1016/j.msec.2014.09.016

Baker BM, Gee AO, Metter RB, Nathan AS, Marklein RA, Burdick JA, Mauck RL (2008) The potential to improve cell infiltration in composite fiber-aligned electrospun scaffolds by the selective removal of sacrificial fibers. Biomaterials 29:2348–2358

Bassiouny HS, White S, Glagov S, Choi E, Giddens DP, Zarins CK (1992) Anastomotic intimal hyperplasia: mechanical injury or flow induced. J Vasc Surg 15:708–716; discussion 716–707

Bastijanic JM, Kligman FL, Marchant RE, Kottke-Marchant K (2016) Dual biofunctional polymer modifications to address endothelialization and smooth muscle cell integration of ePTFE vascular grafts. J Biomed Mater Res A 104:71–81

Bellon J, Bujan J, Contreras L, Hernando A, Jurado F (1996) Similarity in behavior of polytetrafluoroethylene (ePTFE) prostheses implanted into different interfaces. J Biomed Mater Res A 31:1–9

Berger K, Sauvage LR, Rao AM, Wood SJ (1972) Healing of arterial prostheses in man: its incompleteness. Ann Surg 175:118–127

Bezwada R, Jamiolkowski D, Cooper K (1998) Poly-dioxanone and its copolymers. In Handbook of Biodegradable Polymers; Domb, A.J., Kost, J., Wiseman, D.M., Eds.; Hardwood Academic Publishers: Amsterdam. The Netherlands. pp. 29–62

Biela SA, Su Y, Spatz JP, Kemkemer R (2009) Different sensitivity of human endothelial cells, smooth muscle cells and fibroblasts to topography in the nano–micro range. Acta Biomater 5:2460–2466

Biswas A, Bayer IS, Biris AS, Wang T, Dervishi E, Faupel F (2012) Advances in top–down and bottom–up surface nanofabrication: techniques, applications & future prospects. Adv Colloid Interf Sci 170:2–27

Boccafoschi F, Habermehl J, Vesentini S, Mantovani D (2005) Biological performances of collagen-based scaffolds for vascular tissue engineering. Biomaterials 26:7410–7417

Boland ED, Matthews JA, Pawlowski KJ, Simpson DG, Wnek GE, Bowlin GL (2004) Electrospinning collagen and elastin: preliminary vascular tissue engineering. Front Biosci 9:e32

Boland ED, Coleman BD, Barnes CP, Simpson DG, Wnek GE, Bowlin GL (2005) Electrospinning polydioxanone for biomedical applications. Acta Biomater 1:115–123. https://doi.org/10.1016/j.actbio.2004.09.003

Boretos JW, Pierce WS (1968) Segmented polyurethane: a polyether polymer. An initial evaluation for biomedical applications. J Biomed Mater Res 2:121–130. https://doi.org/10.1002/jbm.820020109

Bos GW, Poot AA, Beugeling T, Van Aken W, Feijen J (1998) Small-diameter vascular graft prostheses: current status. Arch Physiol Biochem 106:100–115

Bose GM (1745) Recherches sur la cause et sur la veritable téorie de l'électricité. J.F. Slomac, Wittenberg

Bowlin GL, Meyer A, Fields C, Cassano A, Makhoul RG, Allen C, Rittgers SE (2001) The persistence of electrostatically seeded endothelial cells lining a small diameter expanded polytetrafluoroethylene vascular graft. J Biomater Appl 16:157–173. https://doi.org/10.1106/NCQT-JFV9-2EQ1-EBGU

Brossollet LJ (1992) Mechanical issues in vascular grafting: a review. Int J Artif Organs 15:579–584

Cai W, Liu L (2008) Shape-memory effect of poly (glycerol-sebacate) elastomer. Mater Lett 62:2171–2173

Caves JM, Kumar VA, Martinez AW, Kim J, Ripberger CM, Haller CA, Chaikof EL (2010) The use of microfiber composites of elastin-like protein matrix reinforced with synthetic collagen in the design of vascular grafts. Biomaterials 31:7175–7182

Chan KL, Khankhel AH, Thompson RL, Coisman BJ, Wong KH, Truslow JG, Tien J (2014) Crosslinking of collagen scaffolds promotes blood and lymphatic vascular stability. J Biomed Mater Res A 102:3186–3195

Chen D, Bei J, Wang S (2000) Polycaprolactone microparticles and their biodegradation. Polym Degrad Stab 67:455–459

Chen QZ et al (2008) Characterisation of a soft elastomer poly(glycerol sebacate) designed to match the mechanical properties of myocardial tissue. Biomaterials 29:47–57. https://doi.org/10.1016/j.biomaterials.2007.09.010

Clowes AW, Kirkman TR, Reidy MA (1986) Mechanisms of arterial graft healing. Rapid transmural capillary ingrowth provides a source of intimal endothelium and smooth muscle in porous PTFE prostheses. Am J Pathol 123:220–230

Coury AJ, Slaikeu PC, Cahalan PT, Stokes KB, Hobot CM (1988) Factors and interactions affecting the performance of polyurethane elastomers in medical devices. J Biomater Appl 3:130–179. https://doi.org/10.1177/088532828800300202

Crapo PM, Wang Y (2010) Physiologic compliance in engineered small-diameter arterial constructs based on an elastomeric substrate. Biomaterials 31:1626–1635. https://doi.org/10.1016/j.biomaterials.2009.11.035

Curtis A, Forrester J, Clark P (1986) Substrate hydroxylation and cell adhesion. J Cell Sci 86:9–24

Cziperle D et al (1991) Albumin impregnated vascular grafts: albumin resorption and tissue reactions. J Cardiovasc Surg 33:407–414

Dahl SL et al (2011) Readily available tissue-engineered vascular grafts. Sci Transl Med 3:68ra69. https://doi.org/10.1126/scitranslmed.3001426

Davidenko N, Bax DV, Schuster CF, Farndale RW, Hamaia SW, Best SM, Cameron RE (2016) Optimisation of UV irradiation as a binding site conserving method for crosslinking collagen-based scaffolds. J Mater Sci Mater Med 27:14

Davids L, Dower T, Zilla P (1999) The lack of healing in conventional vascular grafts. In: Tissue engineering of vascular prosthetic grafts. R.G. Landes, Austin, pp 3–44

de Valence S, Tille J-C, Mugnai D, Mrowczynski W, Gurny R, Möller M, Walpoth BH (2012) Long term performance of polycaprolactone vascular grafts in a rat abdominal aorta replacement model. Biomaterials 33:38–47

Dekker A, Reitsma K, Beugeling T, Bantjes A, Feijen J, Van Aken W (1991) Adhesion of endothelial cells and adsorption of serum proteins on gas plasma-treated polytetrafluoroethylene. Biomaterials 12:130–138

Donovan DL, Schmidt SP, Townshend SP, Njus GO, Sharp WV (1990) Material and structural characterization of human saphenous vein. J Vasc Surg 12:531–537

Doshi J, Reneker DH (1995) Electrospinning process and applications of electrospun fibers. J Electrost 35:151–160

Drury JL, Mooney DJ (2003) Hydrogels for tissue engineering: scaffold design variables and applications. Biomaterials 24:4337–4351

Edwards A, Carson RJ, Bowald S, Quist WC (1995) Development of a microporous compliant small bore vascular graft. J Biomater Appl 10:171–187

Ekaputra AK, Prestwich GD, Cool SM, Hutmacher DW (2008) Combining electrospun scaffolds with electrosprayed hydrogels leads to three-dimensional cellularization of hybrid constructs. Biomacromolecules 9:2097–2103

Formhals A (1934) Process and apparatus for preparing artificial threads. U.S. Patent 1975504A. 2 October 1934

Friedman SG, Lazzaro RS, Spier LN, Moccio C, Tortolani AJ (1995) A prospective randomized comparison of Dacron and polytetrafluoroethylene aortic bifurcation grafts. Surgery 117:7–17

Fung YC (1984) Blood flow in arteries. Springer-Verlag, New York

Gandhi R, Wheeler J, Gregory R (1993) Vascular prosthetics: the Gore-Tex ePTFE stretch graft. Surg Technol Int 2:293–297

Garg K, Sell SA, Madurantakam P, Bowlin GL (2009) Angiogenic potential of human macrophages on electrospun bioresorbable vascular grafts. Biomed Mater 4:031001. https://doi.org/10.1088/1748-6041/4/3/031001
Gilding DK, Reed AM (1979) Biodegradable polymers for use in surgery- polyglycolic/poly(actic acid) homo- and copolymers: 1. Polymer 20:1459–1464
Grassl E, Oegema T, Tranquillo R (2002) Fibrin as an alternative biopolymer to type-I collagen for the fabrication of a media equivalent. J Biomed Mater Res A 60:607–612
Green RM et al (2000) Prosthetic above-knee femoropopliteal bypass grafting: five-year results of a randomized trial. J Vasc Surg 31:417–425
Greenwald S, Berry C (2000) Improving vascular grafts: the importance of mechanical and haemodynamic properties. J Pathol 190:292–299
Greiner A, Wendorff JH (2007) Electrospinning: a fascinating method for the preparation of ultrathin fibers. Angew Chem Int Ed 46:5670–5703
Greisler HP (1982) Arterial regeneration over absorbable prostheses. Arch Surg 117:1425–1431
Greisler HP, Ellinger J, Schwarcz TH, Golan J, Raymond RM, Kim DU (1987) Arterial regeneration over polydioxanone prostheses in the rabbit. Arch Surg 122:715–721
Greisler HP, Endean ED, Klosak JJ, Ellinger J, Dennis JW, Buttle K, Kim DU (1988) Polyglactin 910/polydioxanone bicomponent totally resorbable vascular prostheses. J Vasc Surg 7:697–705
Gunatillake PA, Martin DJ, Meijs GF, McCarthy SJ, Adhikari R (2003) Designing biostable polyurethane elastomers for biomedical implants. Aust J Chem 56:545–557
Gunatillake PA, Mayadunne R, Adhikari R (2006) Recent development in biodegradable synthetic polymers. In: Biotechnology annual review, vol 12. Elsevier Science, Amsterdam, The Netherlands. pp 301–347
Guo J, Zhao M, Ti Y, Wang B (2007) Study on structure and performance of polycarbonate urethane synthesized via different copolymerization methods. J Mater Sci 42:5508–5515
Herring M, Gardner A, Glover J (1978) A single-staged technique for seeding vascular grafts with autogenous endothelium. Surgery 84:498–504
Hess F (1985) History of (MICRO) vascular surgery and the development of small-caliber blood vessel prostheses (with some notes on patency rates and re-endothelialization). Microsurgery 6:59–69
Hoshi RA, Van Lith R, Jen MC, Allen JB, Lapidos KA, Ameer G (2013) The blood and vascular cell compatibility of heparin-modified ePTFE vascular grafts. Biomaterials 34:30–41. https://doi.org/10.1016/j.biomaterials.2012.09.046
Hu Y, Pan X, Zheng J, Ma W, Sun L (2017) In vitro and in vivo evaluation of a coaxial electrospun small caliber vascular graft loaded with heparin and VEGF. Int J Surg 44:244
Huang Z-M, Zhang Y-Z, Kotaki M, Ramakrishna S (2003) A review on polymer nanofibers by electrospinning and their applications in nanocomposites. Compos Sci Technol 63:2223–2253
Jamshidian M, Tehrany EA, Imran M, Jacquot M, Desobry S (2010) Poly-lactic acid: production, application, nanocomposites, and release studies. Compr Rev Food Sci Food Saf 9:552–571
Jeong SI et al (2007) Tissue-engineered vascular grafts composed of marine collagen and PLGA fibers using pulsatile perfusion bioreactors. Biomaterials 28:1115–1122
Jeschke MG, Hermanutz V, Wolf SE, Köveker GB (1999) Polyurethane vascular prostheses decreases neointimal formation compared with expanded polytetrafluoroethylene. J Vasc Surg 29:168–176
Jonas RA, Ziemer G, Schoen FJ, Britton L, Castaneda AR (1988) A new sealant for knitted Dacron prostheses: minimally cross-linked gelatin. J Vasc Surg 7:414–419
Kakisis JD, Liapis CD, Breuer C, Sumpio BE (2005) Artificial blood vessel: the holy grail of peripheral vascular surgery. J Vasc Surg 41:349–354
Kakkos SK et al (2008) Equivalent secondary patency rates of upper extremity Vectra Vascular Access Grafts and transposed brachial-basilic fistulas with aggressive access surveillance and endovascular treatment. J Vasc Surg 47:407–414
Kangac SS, Petsikasac D, Murchana P, Cziperlea DJ, Rena D, Kimd DU, Greislerabc HP (1997) Effects of albumin coating of knitted Dacron grafts on transinterstitial blood loss and tissue ingrowth and incorporation. Cardiovasc Surg 5:184–189

Kempczinski RF, Ramalanjaona GR, Douville C, Silberstein EB (1987) Thrombogenicity of a fibronectin-coated, experimental polytetrafluoroethylene graft. Surgery 101:439–444
Kemppainen JM, Hollister SJ (2010) Tailoring the mechanical properties of 3D-designed poly (glycerol sebacate) scaffolds for cartilage applications. J Biomed Mater Res A 94:9–18. https://doi.org/10.1002/jbm.a.32653
Klinkert P, Post PN, Breslau PJ, van Bockel JH (2004) Saphenous vein versus PTFE for above-knee femoropopliteal bypass. A review of the literature. Eur J Vasc Endovasc Surg 27:357–362. https://doi.org/10.1016/j.ejvs.2003.12.027
Koens M et al (2015) Vascular replacement using a layered elastin-collagen vascular graft in a porcine model: one week patency versus one month occlusion. Organogenesis 11:105–121
Konig G et al (2009) Mechanical properties of completely autologous human tissue engineered blood vessels compared to human saphenous vein and mammary artery. Biomaterials 30:1542–1550
Kottke-Marchant K, Anderson JM, Umemura Y, Marchant RE (1989) Effect of albumin coating on the in vitro blood compatibility of Dacron arterial prostheses. Biomaterials 10:147–155
Kulkarni RK, Moore EG, Hegyeli AF, Leonard F (1971) Biodegradable poly(lactic acid) polymers. J Biomed Mater Res 5:169–181. https://doi.org/10.1002/jbm.820050305
Kumar VA, Caves JM, Haller CA, Dai E, Liu L, Grainger S, Chaikof EL (2013) Acellular vascular grafts generated from collagen and elastin analogs. Acta Biomater 9:8067–8074
Kwon IK, Matsuda T (2005) Co-electrospun nanofiber fabrics of poly (L-lactide-co-ε-caprolactone) with type I collagen or heparin. Biomacromolecules 6:2096–2105
L'Heureux N et al (2006) Human tissue engineered blood vessel for adult arterial revascularization. Nat Med 12:361
Lawton E, Ringwald EL (1989) Physical constants of poly(oxyethylene oxyterephthaloyl)[poly (ethylene terephthalate)]. In: Immergut E (ed) Polymer handbook, 3rd edn. Wiley, New York, pp V101–V105
Lee KW, Wang Y (2011) Elastomeric PGS scaffolds in arterial tissue engineering. J Vis Exp. https://doi.org/10.3791/2691
Lee HB, Kim SS, Khang G (1995) Polymers used as biomaterials. In: The biomedical engineering handbook. CRC Press, Inc
Leong MF, Chan WY, Chian KS (2013) Cryogenic electrospinning: proposed mechanism, process parameters and its use in engineering of bilayered tissue structures. Nanomedicine 8:555–566
Li S, Bhatia S, Hu YL, Shiu YT, Li YS, Usami S, Chien S (2001) Effects of morphological patterning on endothelial cell migration. Biorheology 38:101–108
Li C, Wang F, Douglas G, Zhang Z, Guidoin R, Wang L (2017) Comprehensive mechanical characterization of PLA fabric combined with PCL to form a composite structure vascular graft. J Mech Behav Biomed Mater 69:39–49
Liao I, Moutos FT, Estes BT, Zhao X, Guilak F (2013) Composite three-dimensional woven scaffolds with interpenetrating network hydrogels to create functional synthetic articular cartilage. Adv Funct Mater 23:5833–5839
Linderman S, Araya J, Pathan S, Nelson D, Phaneuf M, Contreras M (2014) A small diameter bioactive prosthetic vascular graft with activated protein C (546.9). FASEB J 28:546.549
Liu H, Ding X, Bi Y, Gong X, Li X, Zhou G, Fan Y (2013) In vitro evaluation of combined sulfated silk fibroin scaffolds for vascular cell growth. Macromol Biosci 13:755–766
Lopes MS, Jardini AL, Filho RM (2012) Poly (lactic acid) production for tissue engineering applications. Process Eng 42:1402–1413
Lowery JL, Datta N, Rutledge GC (2010) Effect of fiber diameter, pore size and seeding method on growth of human dermal fibroblasts in electrospun poly (ϵ-caprolactone) fibrous mats. Biomaterials 31:491–504
Marois Y et al (1993) A novel microporous polyurethane vascular graft: in vivo evaluation of the UTA prosthesis implanted as infra-renal aortic substitute in dogs. J Investig Surg 6:273–288
Martz H et al (1988) Hydrophilic microporous polyurethane versus expanded PTFE grafts as substitutes in the carotid arteries of dogs. A limited study. J Biomed Mater Res A 22:63–69

Mathews A, Colombus S, Krishnan VK, Krishnan LK (2012) Vascular tissue construction on poly (ε-caprolactone) scaffolds by dynamic endothelial cell seeding: effect of pore size. J Tissue Eng Regen Med 6:451–461

Matsuda T, Nakayama Y (1996) Surface microarchitectural design in biomedical applications: in vitro transmural endothelialization on microporous segmented polyurethane films fabricated using an excimer laser. J Biomed Mater Res 31:235–242. https://doi.org/10.1002/(SICI)1097-4636(199606)31:2<235::AID-JBM10>3.0.CO;2-K

McClure MJ, Wolfe PS, Simpson DG, Sell SA, Bowlin GL (2012) The use of air-flow impedance to control fiber deposition patterns during electrospinning. Biomaterials 33:771–779

McKenna KA et al (2012) Mechanical property characterization of electrospun recombinant human tropoelastin for vascular graft biomaterials. Acta Biomater 8:225–233

Melchiorri AJ, Hibino N, Fisher JP (2013) Strategies and techniques to enhance the in situ endothelialization of small-diameter biodegradable polymeric vascular grafts. Tissue Eng Part B Rev 19:292–307

Miller DC, Thapa A, Haberstroh KM, Webster TJ (2004) Endothelial and vascular smooth muscle cell function on poly (lactic-co-glycolic acid) with nano-structured surface features. Biomaterials 25:53–61

Min B-M, Jeong L, Nam YS, Kim J-M, Kim JY, Park WH (2004) Formation of silk fibroin matrices with different texture and its cellular response to normal human keratinocytes. Int J Biol Macromol 34:223–230

Nam YS, Yoon JJ, Lee JG, Park TG (1999) Adhesion behaviours of hepatocytes cultured onto biodegradable polymer surface modified by alkali hydrolysis process. J Biomater Sci Polym Ed 10:1145–1158

Narayan D, Venkatraman SS (2008) Effect of pore size and interpore distance on endothelial cell growth on polymers. J Biomed Mater Res A 87:710–718. https://doi.org/10.1002/jbm.a.31749

Pachence J, Kohn J (1997) Biodegrable polymers for tissue engineering. In: Lanza R, Langer R, Chick W (eds) Principles of tissue engineering. RG Lands Company, Georgetown

Pan Y et al (2017) Small-diameter hybrid vascular grafts composed of polycaprolactone and polydioxanone fibers. Sci Rep 7:3615

Patel A, Fine B, Sandig M, Mequanint K (2006) Elastin biosynthesis: the missing link in tissue-engineered blood vessels. Cardiovasc Res 71:40–49

Pathiraja AG, Adhikari R (2003) Biodegradable synthetic polymers for tissue engineering. Eur Cell Mater 5:1–16

Pavot V et al (2014) Poly (lactic acid) and poly (lactic-co-glycolic acid) particles as versatile carrier platforms for vaccine delivery. Nanomedicine 9:2703–2718

Pektok E, Nottelet B, Tille JC, Gurny R, Kalangos A, Moeller M, Walpoth BH (2008) Degradation and healing characteristics of small-diameter poly(epsilon-caprolactone) vascular grafts in the rat systemic arterial circulation. Circulation 118:2563–2570. https://doi.org/10.1161/CIRCULATIONAHA.108.795732

Perego G, Cella GD, Bastioli C (1996) Effect of molecular weight and crystallinity on poly(lactic acid) mechanical properties. Appl Polym Sci 59:37–43

Peters T Jr (1995) All about albumin: biochemistry, genetics, and medical applications. Academic Press. San Diego, California. https://doi.org/10.1016/B978-0-12-552110-9.X5000-4

Pfeiffer D et al (2014) Endothelialization of electrospun polycaprolactone (PCL) small caliber vascular grafts spun from different polymer blends. J Biomed Mater Res A 102:4500–4509

Polterauer P, Prager M, Hölzenbein T, Karner J, Kretschmer G, Schemper M (1992) Dacron versus polytetrafluoroethylene for Y-aortic bifurcation grafts: a six-year prospective, randomized trial. Surgery 111:626–633

Post S et al (2001) Dacron vs polytetrafluoroethylene grafts for femoropopliteal bypass: a prospective randomised multicentre trial. Eur J Vasc Endovasc Surg 22:226–231

Prager M et al (2001) Collagen versus gelatin-coated Dacron versus stretch polytetrafluoroethylene in abdominal aortic bifurcation graft surgery: results of a seven-year prospective, randomized multicenter trial. Surgery 130:408–414

Quarmby J, Burnand K, Lockhart S, Donald A, Sommerville K, Jamieson C, Browse N (1998) Prospective randomized trial of woven versus collagen-impregnated knitted prosthetic Dacron grafts in aortoiliac surgery. Br J Surg 85:775–777

Ramsey W, Hertl W, Nowlan E, Binkowski N (1984) Surface treatments and cell attachment. In Vitro Cell Dev Biol Plant 20:802–808

Ravari H, Kazemzade GH, Modaghegh MHS, Khashayar P (2010) Patency rate and complications of polytetrafluoroethylene grafts compared with polyurethane grafts for hemodialysis access. Ups J Med Sci 115:245–248

Reneker DH, Chun I (1996) Nanometre diameter fibres of polymer, produced by electrospinning. Nanotechnology 7:216

Rhodes JM, Simons M (2007) The extracellular matrix and blood vessel formation: not just a scaffold. J Cell Mol Med 11:176–205. https://doi.org/10.1111/j.1582-4934.2007.00031.x

Row S, Peng H, Schlaich EM, Koenigsknecht C, Andreadis ST, Swartz DD (2015) Arterial grafts exhibiting unprecedented cellular infiltration and remodeling in vivo: the role of cells in the vascular wall. Biomaterials 50:115–126

Ruoslahti E (1996) RGD and other recognition sequences for integrins. Annu Rev Cell Dev Biol 12:697–715. https://doi.org/10.1146/annurev.cellbio.12.1.697

Salacinski HJ, Goldner S, Giudiceandrea A, Hamilton G, Seifalian AM, Edwards A, Carson RJ (2001) The mechanical behavior of vascular grafts: a review. J Biomater Appl 15:241–278

Santerre J, Labow R, Duguay D, Erfle D, Adams G (1994) Biodegradation evaluation of polyether and polyester-urethanes with oxidative and hydrolytic enzymes. J Biomed Mater Res A 28:1187–1199

Sarkar S, Schmitz-Rixen T, Hamilton G, Seifalian AM (2007) Achieving the ideal properties for vascular bypass grafts using a tissue engineered approach: a review. Med Biol Eng Comput 45:327–336

Sauvage LR, Berger KE, Wood SJ, Yates SG 2nd, Smith JC, Mansfield PB (1974) Interspecies healing of porous arterial prostheses: observations, 1960 to 1974. Arch Surg 109:698–705

Scott S, Gaddy L, Sahmel R, Hoffman H (1987) A collagen coated vascular prosthesis. J Cardiovasc Surg 28:498–504

Seifalian AM, Salacinski HJ, Tiwari A, Edwards A, Bowald S, Hamilton G (2003) In vivo biostability of a poly (carbonate-urea) urethane graft. Biomaterials 24:2549–2557

Seifu DG, Purnama A, Mequanint K, Mantovani D (2013) Small-diameter vascular tissue engineering. Nat Rev Cardiol 10:410–421

Selders GS, Fetz AE, Speer SL, Bowlin GL (2016) Fabrication and characterization of air-impedance electrospun polydioxanone templates. Electrospinning 1:20–30

Shalaby S (1996) Classes of materials used in medicine: fabrics. In: Ratner B (ed) Biomaterials science, an introduction to materials in medicine. Academic, San Diego, pp 118–124

Simonet M, Schneider OD, Neuenschwander P, Stark WJ (2007) Ultraporous 3D polymer meshes by low-temperature electrospinning: use of ice crystals as a removable void template. Polym Eng Sci 47:2020–2026

Sivalingam G, Karthik R, Madras G (2003) Kinetics of thermal degradation of poly (ε-caprolactone). J Anal Appl Pyrolysis 70:631–647

Sivalingam G, Vijayalakshmi S, Madras G (2004) Enzymatic and thermal degradation of poly (ε-caprolactone), poly (D, L-lactide), and their blends. Ind Eng Chem Res 43:7702–7709

Smith MJ, McClure MJ, Sell SA, Barnes CP, Walpoth BH, Simpson DG, Bowlin GL (2008) Suture-reinforced electrospun polydioxanone–elastin small-diameter tubes for use in vascular tissue engineering: a feasibility study. Acta Biomater 4:58–66

Soldani G et al (2010) Long term performance of small-diameter vascular grafts made of a poly (ether) urethane–polydimethylsiloxane semi-interpenetrating polymeric network. Biomaterials 31:2592–2605

Soletti L, Hong Y, Guan J, Stankus JJ, El-Kurdi MS, Wagner WR, Vorp DA (2010) A bilayered elastomeric scaffold for tissue engineering of small diameter vascular grafts. Acta Biomater 6:110–122. https://doi.org/10.1016/j.actbio.2009.06.026

Soto M, Sebastián RM, Marquet J (2014) Photochemical activation of extremely weak nucleophiles: highly fluorinated urethanes and polyurethanes from polyfluoro alcohols. J Org Chem 79:5019–5027

Sottiurai VS, Yao JS, Flinn WR, Batson RC (1983) Intimal hyperplasia and neointima: an ultrastructural analysis of thrombosed grafts in humans. Surgery 93:809–817

Sottiurai VS, Sue SL, Feinberg EL 2nd, Bringaze WL, Tran AT, Batson RC (1988) Distal anastomotic intimal hyperplasia: biogenesis and etiology. Eur J Vasc Surg 2:245–256

Stankus JJ, Guan J, Fujimoto K, Wagner WR (2006) Microintegrating smooth muscle cells into a biodegradable, elastomeric fiber matrix. Biomaterials 27:735–744

Stanley JC, Graham L, Glover J (1986) Endothelial cell seeded synthetic vascular grafts. In: Vascular graft update: safety and performance. ASTM, Philadelphia, pp 33–43

Stekelenburg M, Rutten MC, Snoeckx LH, Baaijens FP (2009) Dynamic straining combined with fibrin gel cell seeding improves strength of tissue-engineered small-diameter vascular grafts. Tissue Eng Part A 15:1081–1089. https://doi.org/10.1089/ten.tea.2008.0183

Stewart SF, Lyman DJ (1992) Effects of a vascular graft/natural artery compliance mismatch on pulsatile flow. J Biomech 25:297–310

Sugiura T et al (2016) Novel bioresorbable vascular graft with sponge-type scaffold as a small-diameter arterial graft. Ann Thorac Surg 102:720–727. https://doi.org/10.1016/j.athoracsur.2016.01.110

Sugiura T et al (2017) Fast-degrading bioresorbable arterial vascular graft with high cellular infiltration inhibits calcification of the graft. J Vasc Surg 66:243–250

Sundback CA, Shyu JY, Wang Y, Faquin WC, Langer RS, Vacanti JP, Hadlock TA (2005) Biocompatibility analysis of poly(glycerol sebacate) as a nerve guide material. Biomaterials 26:5454–5464. https://doi.org/10.1016/j.biomaterials.2005.02.004

Syedain ZH, Meier LA, Lahti MT, Johnson SL, Tranquillo RT (2014) Implantation of completely biological engineered grafts following decellularization into the sheep femoral artery. Tissue Eng Part A 20:1726–1734. https://doi.org/10.1089/ten.TEA.2013.0550

Syedain Z, Reimer J, Lahti M, Berry J, Johnson S, Tranquillo RT (2016) Tissue engineering of acellular vascular grafts capable of somatic growth in young lambs. Nat Commun 7, 12951

Syedain ZH, Graham ML, Dunn TB, O'Brien T, Johnson SL, Schumacher RJ, Tranquillo RT (2017) A completely biological "off-the-shelf" arteriovenous graft that recellularizes in baboons. Sci Transl Med 9. https://doi.org/10.1126/scitranslmed.aan4209

Teebken OE, Pichlmaier AM, Haverich A (2001) Cell seeded decellularised allogeneic matrix grafts and biodegradable polydioxanone-prostheses compared with arterial autografts in a porcine model. Eur J Vasc Endovasc Surg 22:139–145. https://doi.org/10.1053/ejvs.2001.1403

Tillman BW, Yazdani SK, Lee SJ, Geary RL, Atala A, Yoo JJ (2009) The in vivo stability of electrospun polycaprolactone-collagen scaffolds in vascular reconstruction. Biomaterials 30:583–588

Tiwari A, Salacinski HJ, Hamilton G, Seifalian AM (2001) Tissue engineering of vascular bypass grafts: role of endothelial cell extraction. Eur J Vasc Endovasc Surg 21:193–201. https://doi.org/10.1053/ejvs.2001.1316

Tomizawa Y (2014) Late spontaneous nonanastomotic transgraft hemorrhage from biological material-impregnated fabric vascular graft may be due to autologous tissue detachment: a clinical hypothesis. Artif Organs 38:1058–1060

Torikai K et al (2008) A self-renewing, tissue-engineered vascular graft for arterial reconstruction. J Thorac Cardiovasc Surg 136:37–45.e31

Ulery BD, Nair LS, Laurencin CT (2011) Biomedical applications of biodegradable polymers. J Polym Sci B Polym Phys 49:832–864. https://doi.org/10.1002/polb.22259

Uttayarat P, Toworfe GK, Dietrich F, Lelkes PI, Composto RJ (2005) Topographic guidance of endothelial cells on silicone surfaces with micro-to nanogrooves: orientation of actin filaments and focal adhesions. J Biomed Mater Res A 75:668–680

Uttayarat P, Chen M, Li M, Allen FD, Composto RJ, Lelkes PI (2008) Microtopography and flow modulate the direction of endothelial cell migration. Am J Phys Heart Circ Phys 294:H1027–H1035

Uttayarat P et al (2010) Micropatterning of three-dimensional electrospun polyurethane vascular grafts. Acta Biomater 6:4229–4237

van Wachem PB, Stronck JW, Koers-Zuideveld R, Dijk F, Wildevuur CR (1990) Vacuum cell seeding: a new method for the fast application of an evenly distributed cell layer on porous vascular grafts. Biomaterials 11:602–606

Vroman L, Adams AL (1969) Identification of rapid changes at plasma–solid interfaces. J Biomed Mater Res A 3:43–67

Walpoth BH, Bowlin GL (2005) The daunting quest for a small diameter vascular graft. Expert Rev Med Devices 2:647–651. https://doi.org/10.1586/17434440.2.6.647

Wang Y, Ameer GA, Sheppard BJ, Langer R (2002) A tough biodegradable elastomer. Nat Biotechnol 20:602–606

Wang X, Lin P, Yao Q, Chen C (2007) Development of small-diameter vascular grafts. World J Surg 31:682–689

Wang K, Xu M, Zhu M, Su H, Wang H, Kong D, Wang L (2013) Creation of macropores in electrospun silk fibroin scaffolds using sacrificial PEO-microparticles to enhance cellular infiltration. J Biomed Mater Res A 101:3474–3481

Weinberg CB, Bell E (1986) A blood vessel model constructed from collagen and cultured vascular cells. Science 231:397–400

Williamson MR, Black R, Kielty C (2006) PCL–PU composite vascular scaffold production for vascular tissue engineering: attachment, proliferation and bioactivity of human vascular endothelial cells. Biomaterials 27:3608–3616

Wise SG, Byrom MJ, Waterhouse A, Bannon PG, Ng MK, Weiss AS (2011) A multilayered synthetic human elastin/polycaprolactone hybrid vascular graft with tailored mechanical properties. Acta Biomater 7:295–303

Wong CS, Liu X, Xu Z, Lin T, Wang X (2013) Elastin and collagen enhances electrospun aligned polyurethane as scaffolds for vascular graft. J Mater Sci Mater Med 24:1865–1874

Woodruff MA, Hutmacher DW (2010) The return of a forgotten polymer – polycaprolactone in the 21st century. Prog Polym Sci 35:1217–1256

World Health Organization (2013) A global brief on hypertension: silent killer, global public health crisis: World Health Day 2013. WHO Press. Geneva, Switzerland

Xie X, Eberhart A, Guidoin R, Marois Y, Douville Y, Zhang Z (2010) Five types of polyurethane vascular grafts in dogs: the importance of structural design and material selection. J Biomater Sci Polym Ed 21:1239–1264

Xie Y, Guan Y, Kim S-H, King MW (2016) The mechanical performance of weft-knitted/electrospun bilayer small diameter vascular prostheses. J Mech Behav Biomed Mater 61:410–418

Xue L, Greisler HP (2003) Biomaterials in the development and future of vascular grafts. J Vasc Surg 37:472–480

Yamada H (1970) Mechanical properties of circulatory organs and tissues. In: Evans FG (ed) Strength of biological materials. Robert E. Krieger, New York, pp 106–137

Yamashita Y (2007) Electrospining the latest in nanotechnology – The creative of nanofibers. Sen-i sha, Osaka

Yates SG et al (1978) The preclotting of porous arterial prostheses. Ann Surg 188:611–622

Yin A, Luo R, Li J, Mo X, Wang Y, Zhang X (2017) Coaxial electrospinning multicomponent functional controlled-release vascular graft: optimization of graft properties. Colloids Surf B: Biointerfaces 152:432–439

You Y, Min BM, Lee SJ, Lee TS, Park WH (2005) In vitro degradation behavior of electrospun polyglycolide, polylactide, and poly (lactide-co-glycolide). J Appl Polym Sci 95:193–200

Yuan X, Mak AF, Yao K (2003) Surface degradation of poly (L-lactic acid) fibres in a concentrated alkaline solution. Polym Degrad Stab 79:45–52

Zhang Z et al (1997) Vascugraft® polyurethane arterial prosthesis as femoro-popliteal and femoro-peroneal bypasses in humans: pathological, structural and chemical analyses of four excised grafts. Biomaterials 18:113–124

Zhu Y, Gao C, Liu X, Shen J (2002) Surface modification of polycaprolactone membrane via aminolysis and biomacromolecule immobilization for promoting cytocompatibility of human endothelial cells. Biomacromolecules 3:1312–1319

Zhu Y, Cao Y, Pan J, Liu Y (2010) Macro-alignment of electrospun fibers for vascular tissue engineering. J Biomed Mater Res B Appl Biomater 92:508–516

Zhu M et al (2015) Circumferentially aligned fibers guided functional neoartery regeneration in vivo. Biomaterials 61:85–94. https://doi.org/10.1016/j.biomaterials.2015.05.024

Zilla P, Bezuidenhout D, Human P (2007) Prosthetic vascular grafts: wrong models, wrong questions and no healing. Biomaterials 28:5009–5027. https://doi.org/10.1016/j.biomaterials.2007.07.017

Zorlutuna P, Rong Z, Vadgama P, Hasirci V (2009) Influence of nanopatterns on endothelial cell adhesion: enhanced cell retention under shear stress. Acta Biomater 5:2451–2459